INORGANIC CHEMISTRY FRONTIERS

REVIEW

View Article Online
View Journal | View Issue

Cite this: *Inorg. Chem. Front.*, 2023, **10**, 5225

Recent developments and prospects for engineering first-row transition metal-based catalysts for electrocatalytic NO_x^- reduction to ammonia

Yi Feng,[a] Lei Chen[a] and Zhong-Yong Yuan *[a,b]

Immense interest in the electrocatalytic reduction of nitrate (NO_3^-)/nitrite (NO_2^-) to ammonia has been driven by promising prospects as an eco-friendly and energy-efficient approach for wastewater treatment and ammonia synthesis. Currently, a variety of transition metal-based catalysts have been developed, but these still suffer from inferior selectivity and low energy conversion efficiency. Among diverse transition metal-based catalysts, first-row transition metal-based catalysts exhibit the advantages of suitable adsorption energies for NO_x^- species and high abundance. As a consequence, this review firstly discusses the reaction mechanisms and hurdles for reaching high-efficiency NH_3 production and analyses the principles for constructing superior NO_x^- reduction catalysts. Then, the focus of this review is placed on recent advances in first-row transition metal-based electrocatalysts, including Cu, Fe, Co, Ni, Ti-based electrocatalysts, for electrochemical NO_3^-/NO_2^- reduction. Finally, the challenges and opportunities are highlighted for future studies and applications. This review provides novel perspectives and ideas for developing first-row transition metal-based NO_x^- reduction electrocatalysts.

Received 13th June 2023,
Accepted 14th July 2023

DOI: 10.1039/d3qi01113e

rsc.li/frontiers-inorganic

1. Introduction

Ammonia (NH_3) exerts a significant influence on economic development and demographic growth.[1–3] NH_3 currently accounts for approximately 5% of the market value of chemicals, occupying a market size reaching 175 million tons and a market value approaching $67 billion.[4] Lim *et al.* have speculated that with the global population growing on a moderate fecundity assumption model, the market size of NH_3 could reach 220–402 million tons in 2050, while the market value would expand to $374–$495 billion.[5] However, current ammonia production is primarily dependent on the Haber–Bosch process. The Haber–Bosch process is characterized by high energy consumption (5.5 EJ yr^{-1}), accompanied by significant carbon dioxide emissions exceeding 450 million metric tons per year.[6] Apparently, with the unceasing employment of the industrial Haber–Bosch route for NH_3 production, the global energy crisis will inevitably be aggravated and the achievement of carbon neutrality will be hindered. In order to achieve a flourishing ammonia economy, it is highly imperative to explore alternative routes for sustainable ammonia production.

Among these alternative approaches, the electrocatalytic reduction of N-containing species has emerged as an attractive approach under ambient conditions on account of its appealing cost and environmental friendliness.[7] The advantages of electrocatalytic ammonia production compared to the Haber–Bosch process ($N_2 + 3H_2 = 2NH_3$) include the following two points: (1) It is operated under ambient conditions, which avoids the high temperature (>450 °C) and high pressure (>10 MPa) conditions of the Haber–Bosch process.[8] (2) It is more conducive to achieving carbon neutrality due to the elimination of massive CO_2 production. However, since aqueous phase conditions are usually adopted for electrocatalytic ammonia production, it is difficult to escape competition from the hydrogen evolution reaction (HER).[9] In addition, the lack of prominent catalysts results in large-scale electrocatalytic ammonia production with uncompetitive cost and inferior efficiency compared to the sufficiently mature Haber–Bosch process in industry. For example, the aqueous electrochemical N_2 reduction reaction (NRR) has been extensively studied under laboratory conditions,[10] but currently reported aqueous NRR experiments are limited by low NH_3 yield (10^{-11} mol cm^{-2} s^{-1}) and an undesirable faradaic efficiency (FE) below

[a]*National Institute for Advanced Materials, School of Materials Science and Engineering, Smart Sensing Interdisciplinary Science Center, Nankai University, Tianjin 300350, China. E-mail: zyyuan@nankai.edu.cn*
[b]*Key Laboratory of Advanced Energy Materials Chemistry (Ministry of Education), Nankai University, Tianjin 300071, China*

20%.[11] The bleak performance of the aqueous NRR system is apparently insufficient to realize sustainable ammonia production.[12]

Recently, the electrocatalytic nitrate (NO_3^-)/nitrite (NO_2^-) reduction reaction has shed new light on renewable NH_3 synthesis as NO_x^- exhibits substantially increased solubility in water and lower cleavage energy compared to N_2.[13–15] The stable supply of NO_3^- and NO_2^- is a crucial factor for achieving electrocatalytic green ammonia generation. It might be advisable to obtain NO_x^- from wastewater.[16] The enrichment of NO_x^- in ground water is primarily caused by the runoff of artificial nitrogenous fertilizers and acid rain formed by nitrogen oxides emitted from factories and automobiles, which results in jeopardized public health, devastated aquatic ecosystems and disturbed global nitrogen cycle.[17] Indeed, the electrocatalytic reduction of NO_x^- to produce NH_3 is also a favorable avenue for removing NO_x^- pollution and restoring the global nitrogen cycle.[18] Compared with the most widely employed conventional biotechnology constrained by prohibitive start-up costs and cumbersome technical procedures,[19] the electrocatalytic reduction of NO_x^- to NH_3 holds a more favourable prospect for the treatment of NO_3^- and NO_2^- in wastewater, due to its uncomplicated operating conditions, excellent efficiency and appealing products. However, for direct electrocatalytic reduction or advanced collection of NO_x^- from wastewater, it is difficult to escape from the effects of unknown NO_x^- concentration, other ions and pH of the solution.[20,21] Time-consuming and labor-intensive wastewater pretreatment is required due to the numerous unknown factors of wastewater, which hinder the realization of electrocatalytic NH_3 production.

In addition to gaining NO_3^- from wastewater, the electrocatalytic oxidation of N_2 to produce NO_3^- opens up novel insights into the green industrial synthesis of NO_3^- and restoration of the global nitrogen cycle.[22] Diverse electrocatalysts including Fe–SnO_2 [23] and $Pd_{0.9}Ru_{0.1}O_2$ [24] have been developed for the electrooxidation of N_2 to NO_3^- over the past three years. However, accelerating the complex five-electron transfer process and breaking the robust N≡N bonds remain major bottlenecks for the development of this technology.[25]

With regard to electrocatalytic NO_x^- reduction reactions, they are multi-step processes involving multiple electron/proton transfers and complex intermediate evolution.[26] Moreover, NO_x^- reduction reactions face the challenge of competing with other side reactions under aqueous conditions including the hydrogen evolution reaction (HER).[27] Consequently, considerable efforts are currently being spent on exploring highly selective and active catalysts for the electrocatalytic reduction of NO_x^- to NH_3, including noble-metal catalysts,[28,29] single-atom catalysts,[30] transition metal-based compounds,[31] non-metal-based nanomaterials.[32]

The number of publications during the past decade on different elements applied to the electrocatalytic reduction of NO_x^- to NH_3 according to the Web of Science database are illustrated in Fig. 1. Obviously, first-row transition metals including Ti, Fe, Co, Ni and Cu have gained broad attention

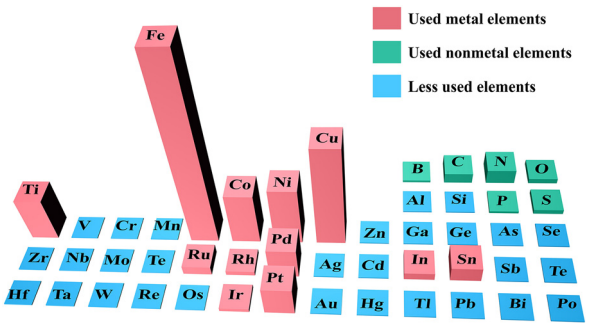

Fig. 1 Publications on various elements for NO_x^- reduction in the last decade (the height of the column is positively correlated with the number of relevant publications).

due to their affordability and easily tunable structures. Some reviews focus on NO_3^- reduction,[33–35] but few contributions concentrate on NO_2^- reduction to NH_3. Indeed, NO_2^- is more easily reduced compared to NO_3^-, and NO_3^- in the natural environment is also easily transformed into NO_2^- by microorganisms.[36]

Hence, this review summarizes the recent progress of studies on first-row transition metal-based electrocatalysts for aqueous NO_3^-/NO_2^- reduction to NH_3 under ambient conditions. This review firstly presents a brief demonstration of the differences in mechanisms of NO_3^- and NO_2^- reduction, while hurdles and corresponding strategies are analysed toward electrocatalytic NO_x^- reduction to NH_3. Then, the focus is placed on recent advances in first-row transition metal-based electrocatalysts, including Cu, Fe, Co, Ni, and Ti-based electrocatalysts, for electrochemical NO_3^-/NO_2^- reduction. Finally, the challenges and opportunities for future studies and applications are discussed with the aim of shedding light on the preparation of highly active and selective transition metal-based electrocatalysts for electrochemical NO_3^-/NO_2^- reduction.

2. Reaction mechanisms of electrocatalytic NO_x^- reduction to ammonia

2.1. Reaction mechanisms

Recognizing and mastering the mechanisms of the electrocatalytic conversions of NO_3^- and NO_2^- to NH_3 are a prerequisite for exploring highly selective and active electrocatalysts. The electrochemical reduction of NO_3^- is a complex process with multielectron reactions,[37] which involve various nitrogen-containing intermediates and products ranging from −3 to +5 valence states. N_2 and NH_3/NH_4^+ are widely recognized as the most thermodynamically stable products,[26] but the final result can be altered for several reasons, such as cathode materials and the pH value of the solution. The indirect autocatalytic reduction mechanism and the direct electrocatalytic reduction mechanism comprise the currently accepted mechanisms of

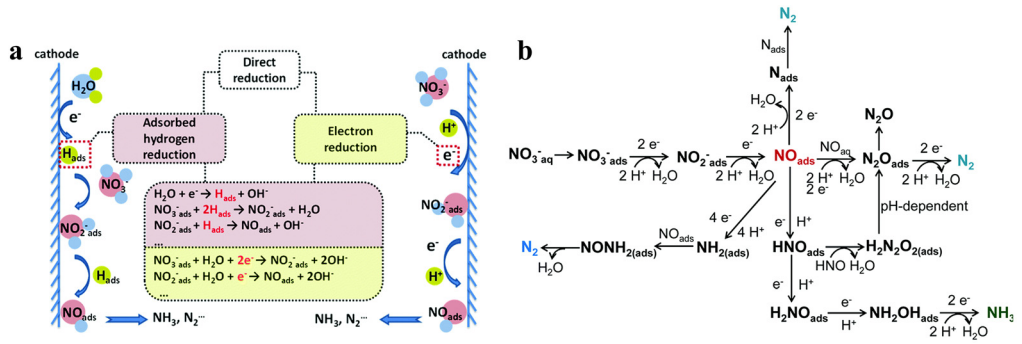

Fig. 2 (a) The proposed direct and indirect pathways of nitrate electroreduction. (b) The electron-mediated pathway of nitrate electroreduction copied with permission.[38] Copyright 2021, Royal Society of Chemistry.

NO_3^- electroreduction.[38] The conversion of NO_3^- to NH_3 generally follows the direct electrocatalytic reduction mechanism occurring in alkaline media with comparatively low concentrations of NO_3^-.[39] The active adsorbed hydrogen atom (H_{ads})-mediated route and the electron-mediated pathway are pursued simultaneously in the direct mechanism (Fig. 2a), which leads to the complexity of electrocatalytic NO_3^- reduction.

The electroreduction of NO_3^- is initiated by the adsorption of NO_3^- ions onto the cathodic electrodes. Adsorbed NO_3^- is transformed into NO_2^- by a tripartite electrochemical–chemical–electrochemical process, which is the dominant rate-controlling step.[40] Later, the important nitric oxide (NO_{ads}) intermediate is obtained by NO_2^- conversion. As depicted in Fig. 2b, NO_{ads} can be reduced to NH_3 as the ultimate product and occupy a dominant position in the N_2 formation pathway.

In addition, the reduction process of NO_3^- can proceed *via* the intermediate H_{ads}. $NO_2^-{}_{ads}$, NO_3^-, and NO_{ads} can be reduced by H_{ads}.[7] The predominant final product in this H_{ads}-mediated process is ammonia, which is caused by the fact that the formation of N–N bonds mediated by H_{ads} is kinetically more challenging than the formation of N–H bonds. The specific H_{ads}-mediated pathways are described in reactions (1)–(7).

$$H_2O + e^- \rightarrow H_{ads} + OH^- \quad (1)$$

$$NO_3^- + 2H_{ads} \rightarrow NO_{2ads}^- + H_2O \quad (2)$$

$$NO_{2ads}^- + H_{ads} \rightarrow NO_{ads} + OH^- \quad (3)$$

$$NO_{ads} + 2H_{ads} \rightarrow N_{ads} + H_2O \quad (4)$$

$$N_{ads} + H_{ads} \rightarrow NH_{ads} \quad (5)$$

$$NH_{ads} + H_{ads} \rightarrow NH_{2ads} \quad (6)$$

$$NH_{2ads} + H_{ads} \rightarrow NH_{3ads} \quad (7)$$

The electrocatalytic reduction of NO_2^- to NH_3 is roughly identical to the reduction process following the conversion of NO_3^- to NO_2^-.[41] It is worth noting that during the reduction of NO_{ads} generated by NO_2^- to NH_3, NO_2^- may generate hydroxylamine (NH_2OH) as a by-product. This specific reaction is as follows:

$$NO_2^- + 4H^+ + 4e^- \rightarrow NH_2OH + OH^- \quad (8)$$

2.2. Hurdles and strategies for reaching high-efficiency NH_3 production

2.2.1. Selectivity requiring improvement. The various nitrogen-containing products involved in the NO_x^- reduction process were initially discussed in section 2.1. During the NO_x^- reduction process, the hydrogenation path of N_{ads} may be hampered by the coupling reaction with the adjacent N_{ads}, which leads to the production of N_2, N_2H_4 and N_2O, blocking the generation of NH_3. Therefore, avoiding coupling reactions between N_{ads} and N_{ads} is essential to design high selectivity electrocatalysts for NH_3 synthesis. Simultaneously, competition from the HER is also a major obstacle in the process of reducing NO_x^- to ammonia.[34] Although the standard electrode potentials of the NO_x^- reduction reactions are larger than that of the HER (Fig. 3a), it is still difficult to circumvent competition from the HER, which only involves two-electron transfers in an aqueous system.

DFT calculations have been employed to explore the thermodynamics of NH_3 selectivity on different transition metal elements. The Gibbs free energy of N_{ads} ($G_{ad}(N)$) of different transition metal elements is correlated with the Gibbs free energy of the NO_x^- reduction reaction. Fig. 3b and c demonstrates theoretical estimates based on the $G_{ad}(N)$ of various transition metal elements.[41] Cu is more favourable for conducting NORR compared to HER, which simultaneously possesses a suitable adsorption energy scaling relationship. Thereby, Cu is theoretically considered to be a decent catalyst for ammonia production. The selectivity of catalysts can also be affected by different potentials. Liu *et al.* predicted the activity and selectivity for NO_3^- reduction on transition metals at various voltages;[26] this was accomplished by exploring the adsorption energies of O and N atoms under different potentials. The study reveals that catalysts with moderate ΔE_O and ΔE_N are inclined to exhibit more remarkable NH_3 selectivity at higher negative potentials. As shown in Fig. 3d, Co and Rh

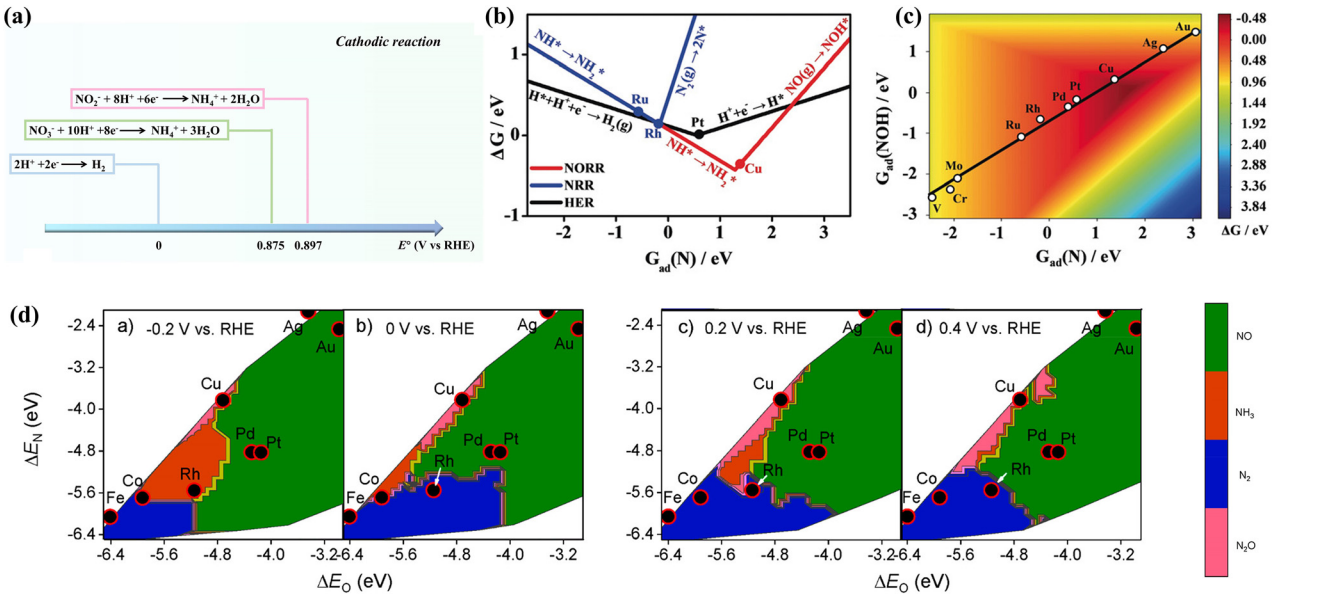

Fig. 3 (a) Comparison of standard reduction potentials for the HER and NO_x^- reduction reactions. (b) Comparison of the ΔG-determining steps between diverse reactions. (c) Activity planar graph for ammonia production copied with permission.[41] Copyright 2020, John Wiley and Sons. (d) Theoretical selectivity maps of various nitrogen-containing products from electrocatalytic NO_3^- reduction on the basis of ΔE_O and ΔE_N under different applied voltages copied with permission.[26] Copyright 2019, American Chemical Society.

demonstrate more outstanding selectivity for ammonia at −0.2 *vs.* RHE.

It is obvious from the above content that the adsorption capacities of N or O-containing species are essential to enhance NH_3 selectivity. According to d-band theory,[42,43] the adsorption energy of intermediates is related to the location of the d-band center of the catalyst. Obviously, ΔE_O and ΔE_N can be modulated by adjusting the d-band center of the catalyst, thus regulating the selectivity of ammonia generation.[44] For example, Cu is doped in Co_3O_4 nanowires to regulate the d band center position of Co_3O_4 due to the interactions between Cu and Co.[45] The density of states reveals that the d-band center position of Cu–Co_3O_4 (−1.57 eV) is downwardly shifted compared to Co_3O_4 (−1.45 eV). Correspondingly, the adsorption energy of $*NO_2$ on the surface of Cu–Co_3O_4 is also reduced compared with that of Co_3O_4. The hydrodeoxygenation free energy of the NO_3^- reduction intermediate is optimized in Cu–Co_3O_4 with an appropriate d-band center position and suitable $*NO_2$ adsorption capacity, and the optimal NO_3^- reduction performance of Cu–Co_3O_4 is also experimentally confirmed to reach a decent yield rate of 36.71 mmol h^{-1} g^{-1} at −0.6 V *vs.* RHE with an excellent FE of 86.5%.

Circumventing the direct coupling of *N is also a valid approach for reducing the generation of N_2 and N_2O by-products and amplifying the NH_3 selectivity. Compared with the inevitable production of N_2O and N_2 by transition metal-based catalysts possessing two adjacent active sites, single-atom metals are more promising for inhibiting the direct coupling of N owing to the absence of adjacent active sites.[46] The isolated Au atoms are distributed into Cu nanoparticles to modify the selectivity and activity of NO_3^- reduction.[29] The introduction of Au single atoms on Cu has been proved to observably accelerate NO_3^- adsorption; the deoxidization process of $*NO_2$ is also boosted due to the formed Au–Cu bond. In addition, more outstanding NH_3 selectivity is obtained for Cu doped with Au single atoms due to the difficult direct coupling of *N on single atoms, reaching remarkable FEs up to 99.69% at −0.80 V *vs.* RHE.

Furthermore, strong competition from the HER is hard to neglect in the aqueous system.[47] However, it is unconscionable to impede the HER by inhibiting the formation of active hydrogen species, since active hydrogen species are indispensable reactants for the subsequent hydrogenation process in NO_x^- reduction. In an environment with sufficient active hydrogen species, employing metal-based catalysts such as Mo and W (Fig. 4c) with difficult release of H_{ads} intermediates may be a decent approach to reduce hydrogen formation and enhance NH_3 selectivity.[48] The strategy of employing two sites can be used for reference to simultaneously realize active hydrogen species production and reduce the direct coupling of active hydrogen species. In this strategy, one site acts as a proton warehouse to promote proton generation, and the other site temporarily stores active hydrogen species for the subsequent hydrogenation reaction.

In addition, the hydrophilicity and aerophobicity of catalysts can also have a bearing on the selectivity of catalysts. The outstanding hydrophilicity of catalysts can accelerate mass transfer in an aqueous system. For example, the super-hydrophilic surface of Fe-based cyano-coordination polymer nanosheets (Fe–cyano NSs) is more conducive to enhancing the contact between the electrolyte and the electrode surface for faster conversion to Fe^0 active sites. Abundant Fe^0 active

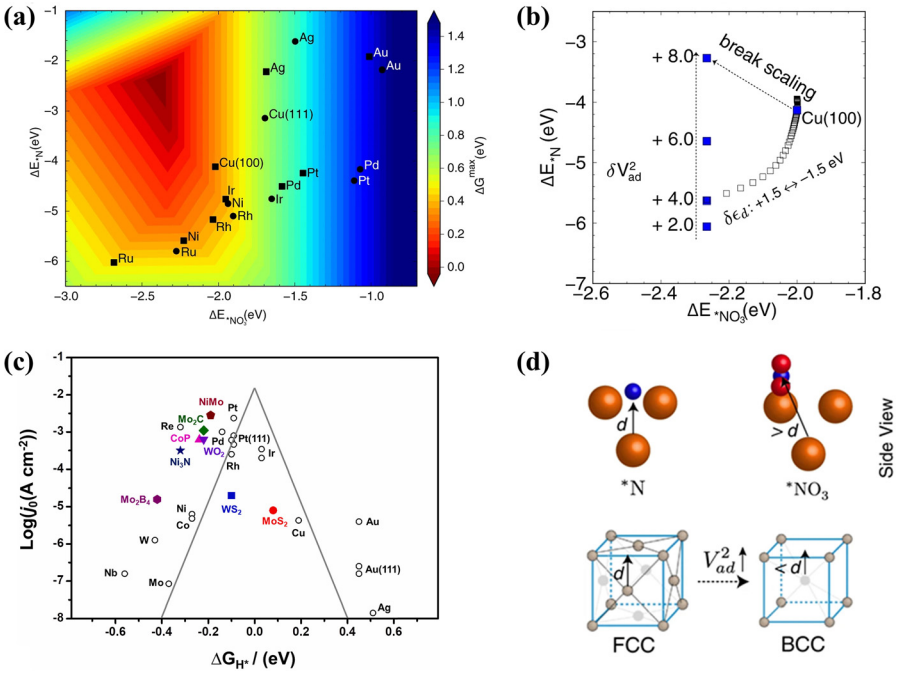

Fig. 4 (a) The activity volcano plot of various metal elements for the conversion of NO_3^- to NH_3. (b) Adsorption energies of $*NO_3$ and *N on Cu (100) under different V^2_{ad}. (d) Models of the (100) facet and the (111) facet copied with permission.[53] Copyright 2022, Springer Nature. (c) The volcano plot of Gibbs free energy of hydrogen (ΔG^*_H) on different metal-based compounds copied with permission.[48] Copyright 2019, Elsevier.

sites in Fe–cyano-R NSs are more favorable for the adsorption of NO_x^- ions.[49] Moreover, considering that the strongly competing reaction with the NO_x^- reduction reaction is the HER, which is accompanied by bubble release, the super-aerophobic nature of a material is more conducive to boosting NO_x^- reduction, which can effectively avoid blockage of the active sites caused by the accumulation and adhesion of gas bubbles on the surface.[50]

2.2.2. Inferior energy conversion efficiency. Although decent selectivity has been shown in the currently developed catalysts, little emphasis has been placed on the undesirable energy conversion efficiency. Indeed, due to the multiple electron transfer processes of NO_x^-, the majority of ammonia-producing systems require considerably negative potentials (<−0.2 V) to exhibit promising performance, accompanied by suboptimal energy consumption (21–38 kW h kg^{-1}).[51] Therefore, it is of major concern to reduce the overpotential in the NO_x^- reduction process, which is tightly related to the energy conversion efficiency of the ammonia production process.

Exploring the factors influencing the activation energy of the elemental reaction is of significance to optimize the overpotential, which is the potential determining step (PDS) in the conversion of NO_x^- to NH_3. Despite the increased adsorption of reactants causing accelerated reactant activity, the dilemma of enhanced activation energy still exists due to the corresponding increase in intermediate adsorption energies restricting the desorption of products. According to Sabatier's principle, scaling relationships between the adsorption energy and activation energy are obstacles to overcome for enhanced reduction activity, causing a volcano plot for the adsorption of reactants in NO_x^- reduction.[52] The design of catalysts with dual active sites is an effective strategy to break the scaling relationships by simultaneously promoting the adsorption of reactants and accelerating the desorption of products. The scaling relationships are broken in Co_3O_4/Cu catalysts with dual active sites, reaching enhanced adsorption of NO_3^- (−2.91 eV) with a low desorption energy barrier for NH_3 (0.13 eV).[45]

Imposing nanoscopic confinement[54] and adjusting strain[55] can also be considered to break scaling relationships. However, constructing strategies based on theoretical guidance is more important for circumventing scaling relationships. The adsorption energies of hollow *N and bridge-bidentate $*NO_3$ are employed as reactivity descriptors for constructing an activity volcano plot of NO_x^- reduction to NH_3 (Fig. 4a).[53] The (100)-oriented B2 CuPd nanocubes are developed with increased $*NO_3$ adsorption and attenuated *N binding; this has been confirmed to break the scaling relationship. The enhanced bridge-bidentate $*NO_3$ adsorption is caused by the upshift of the d-band center position in Cu after introducing Pd. More significantly, regulating the Pauli repulsion between the metallic d-state and the adsorbate frontier orbital has been found to promote the hydrogenation process of hollow *N. As described in Fig. 4b, the adsorption strength of *N at the (100) hollow site increases with the enhancement of the interatomic coupling strength (V^2_{ad}); this is caused by the obtained dominant position of Pauli repulsion with decreasing adsorbate-metal antibonding states. Fig. 4d displays the advantage of the

(100) facet compared to the (111) facet; stronger interatomic coupling can be achieved for the (100) facet due to the closer distance between the subsurface metal–ligand and *N. Hollow *N is more easily destroyed due to the dominant effect of Pauli repulsion, which promotes the hydrogenation of *N to form NH_3. This intriguing strategy can be employed for reference to break the scaling relationship through modifying the Pauli repulsion between the metallic d-state and the adsorbate frontier orbital.

In summary, the design of high-efficiency NO_x^- reduction electrocatalysts requires consideration of selectivity enhancement and overpotential reduction, which are of significant importance for achieving large-scale and green electrocatalytic ammonia production routes. According to the current development of aqueous NO_x^- reduction technology, the following points should be observed when designing electrocatalysts with excellent selectivity and remarkable overpotential. (1) Increasing the adsorption of NO_3^- and NO_2^- on catalysts is beneficial for the reaction. However, the problem of attenuated product desorption should also be taken into account accompanied by enhanced NO_x^- adsorption. It is an important strategy to drastically improve the NO_x^- reduction performance of catalysts though breaking the scaling relationship between the adsorption energies of intermediates and reactants. (2) It is difficult to escape competition from the HER under aqueous conditions. Suppressing the formation of active hydrogen species is unadvisable to reduce HER competition because active hydrogen species are indispensable reactants for the subsequent hydrogenation process in NO_x^- reduction. The strategy of employing two sites can be used for reference to simultaneously realize active hydrogen species production and reduce the direct coupling of active hydrogen species. In this strategy, one site acts as a proton warehouse to promote proton generation, and the other site temporarily stores active hydrogen species for the subsequent hydrogenation reaction. (3) In addition to the HER side reaction, other side reactions generating N_2 or NO should not be ignored. Improved stability of intermediates including $*NO_2$ or *NOH facilitates more efficient ammonia production.

3. First-row transition metal-based electrocatalysts

3.1. The unique advantages of first-row transition metal elements

The development of transition metal-based catalysts is a popular topic due to their low price and controllable structures.[56–58] In accordance with the above exploration of the design principles for NO_x^- reduction catalysts, a promising catalyst should possess moderate interactions with the reactants; either overly weak or excessively strong reactant adsorption is unfavourable for the reaction to proceed. Fig. 5a reveals the adsorption energies of NO_3^- species and protons on transition metal atoms. Obviously, overly strong adsorption strength with NO_3^- species will hinder the production of NH_3 due to dead-end species formation.[59] Therefore, Zr, Hf, W and Re atoms are obviously unsuitable for employment as NO_x^- reduction catalysts. The difference between the adsorption energies of NO_3^- species and protons can provide rough indications of the selectivity degree. Au, Rh, and Ag atoms are found to possess strong adsorption for protons; this is clearly detrimental for escaping competition from the HER. HER competition is likely to be reduced with first-row transition metals, including Ti, Fe, Co, Ni and Cu, which possess more suitable adsorption energies for NO_3^- species and protons. In addition, the unclosed d-orbital shells of first-row transition metals are conducive to the injection of charge into the lowest unoccupied molecular π^* orbital of NO_x^-.[60] The first-row transition metal elements also satisfy the requirements of desirable abundance and competitive costs (Fig. 5b).[61] Since few or no reports are found on the application of V, Cr, and Mn as NO_x^- reduction catalysts, Ti, Fe, Co, Ni and Cu-based catalysts are mainly discussed in this paper.

3.2. Cu-based electrocatalysts

Considerable endeavors have been directed towards the development of Cu-based catalysts (Table 1) with competitive costs and superior intrinsic activity,[53] for example, the alloying of

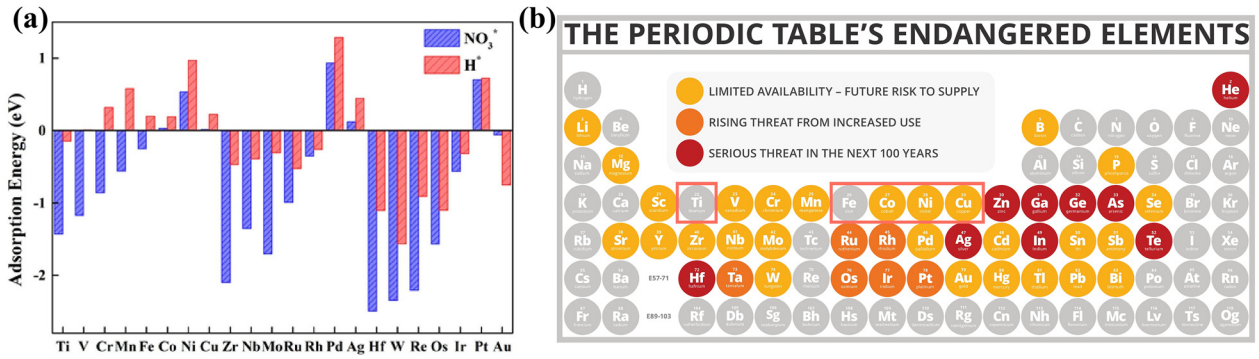

Fig. 5 (a) Adsorption energies for NO_3^- species and protons on different metals copied with permission.[59] Copyright 2022, Elsevier. (b) The predicted elemental content of the periodic table within the next 100 years (gray represents high abundance) copied with permission.[60] Copyright 2021, Elsevier.

Table 1 Summary of NO_x^- reduction performance of Cu-based electrocatalysts

Electrocatalyst	Electrolyte	Potential (V *vs.* RHE)	NH_3 yield	Faradaic efficiency (%)	Ref.
Cu SAC	0.1 M OH^- + 0.1 M NO_3^-	−1.0	4.5 mg cm^{-2} h^{-1}	84.7	104
Cu nanosheets	0.1 M OH^- + 0.1 M NO_3^-	−0.15	390.1 μg mg^{-1} h^{-1}	99.7	105
$Cu_{50}Ni_{50}$ alloy	1 M KOH + 10 mM KNO_3	−0.15	—	99 ± 1	63
$Cu_{50}Co_{50}$	1 M KOH + 100 mM KNO_3	−0.2	4.8 mmol cm^{-2} h^{-1}	100	64
Cu–CuO	0.1 M KOH + 0.1 M NO_3^-	−0.8	3.17 mol h^{-1} g^{-1}	98.7	106
Cu@$Cu_{2+1}O$ nanowires	0.5 M K_2SO_4 + 50 mg L^{-1} NO_3^-	−0.545	3.53 μg h^{-1} mg^{-1}	87.7	107
Cu@TiO_2/TP	0.1 M Na_2SO_4 + 0.1 M NO_2^-	−0.6	760.5 μmol h^{-1} cm^{-2}	95.3	108
CF@Cu_2O	0.1 M PBS + 0.1 M $NaNO_2$		441.8 μmol h^{-1} cm^{-2}	94.2	109
Cu3P NA/CF	0.1 M PBS + 0.1 M $NaNO_2$		95.6 μmol h^{-1} cm^{-2}	91.2	110

Cu.[62] The introduction of other metal elements contributes to modulating the d-band center of Cu and thus regulating the adsorption energies of intermediates. The $Cu_{50}Ni_{50}$ alloy obtained by introducing Ni shows a nitrate reduction activity six times higher than that of pure copper at 0 V.[63] By alloying Ni, the half-wave potential of Cu is shifted upwards by 0.12 V and the adsorption energies of intermediates including $*NO_3$, $*NO_2$ and $*NH_2$ are regulated. The bimetallic electrocatalysts can also synergistically promote the NO_x^- reduction process by combining the advantages of different metals. The CuCo alloy nanosheets exhibit FEs exceeding 90% for ammonia over a wide potential window (from −0.1 to −0.4 V) through emulating the bifunctional nature of nitrite reductase.[64] *H species can be more easily adsorbed by Co, resulting in a decrease in ΔG of the hydrogenation reaction of $*NO_x$. The electronic structure of Cu is also adjusted by introducing Co, which is conducive to reducing the energy barrier of the initial $*NO_3$ adsorption step on Cu. In addition to transition metal elements, combinations of Cu with precious metals to form high-performance alloy catalysts are also not unusual. The CuRu alloy demonstrates a decent nitrate reduction activity and significantly inhibits the production of nitrite.[65] The superior performance of CuRu alloy can be attributed to the synergistic effects between the Ru and Cu sites through relay catalysis. The Cu active sites dramatically promote the reduction of NO_3^- to NO_2^-, while the Ru sites exhibit outstanding activity for the subsequent conversion of NO_2^- to NH_3. However, the cost of producing such bimetallic catalysts is undesirable due to the scarce reserves and prohibitive price of Ru.

Among various Cu-based catalysts, Cu and Cu_2O have been gaining considerable attention. Revealing the reactivity of different exposed facets on Cu and Cu_2O is crucial for investigating the kinetics of NO_x^- reduction and designing catalysts with superior performance. The NO_3^- reduction behaviour of the (111), (100) and (110) facets on Cu is probed, while competition from the HER on various facets is also investigated at different pH values (Fig. 6a).[66] Theoretical calculations

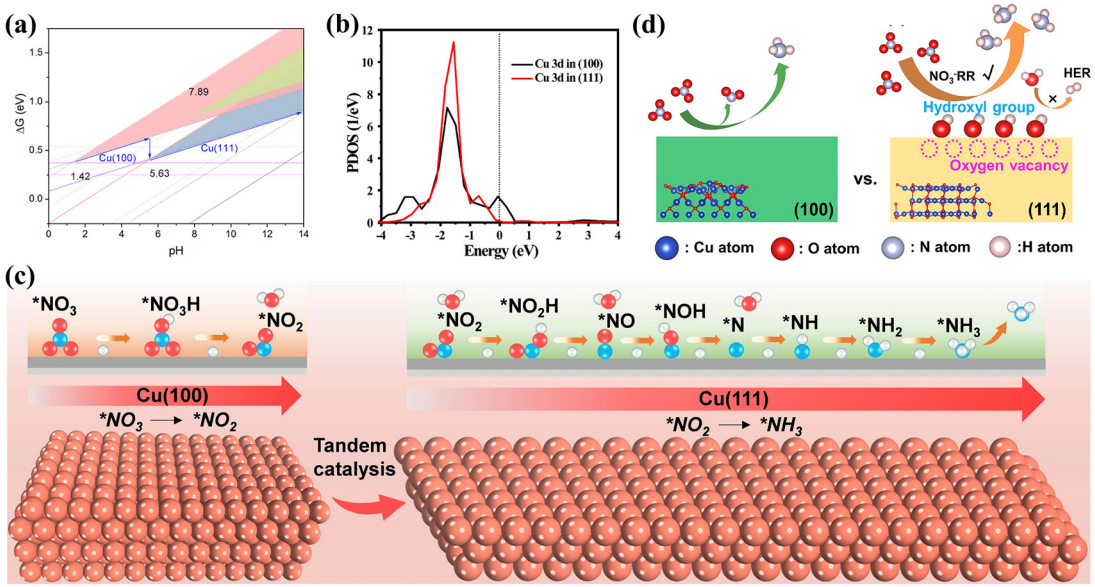

Fig. 6 (a) Comparison of different facets under various pH conditions copied with permission.[66] Copyright 2021, American Chemical Society. (b) Projected density of states of Cu 3d states on different Cu_2O surfaces copied with permission.[67] Copyright 2022, American Chemical Society. (c) Tandem catalytic process of Cu(100) and Cu(111) surfaces copied with permission.[69] Copyright 2023, John Wiley and Sons. (d) Effects of surface oxygen species on the NO_3^- reduction process at different surfaces of Cu_2O copied with permission.[71] Copyright 2023, Elsevier.

confirm the strongest contribution from the (100) and (111) facets in the reduction of NO_3^- to NH_3, excluding the (110) face. The Cu(111) surface exhibits the greatest NO_3^- to NH_3 performance in near-neutral and alkaline environments, while the Cu(100) surface demonstrates better performance in strongly acidic environments. The effects of Cu_2O(100) and (111) surfaces on NO_3^- reduction are also explored. The higher NH_3 yield of 743 μg h^{-1} mg_{cat}^{-1} on the Cu_2O(100) surface is attributed to the partially unfilled Cu 3d state possessed by the (100) facet (Fig. 6b), simultaneously accepting electrons from Cu_2O and combining with NO_x^-. In contrast, the excess filling of the Cu 3d state on the (111) surface inhibits the formation of NH_3.[67] Based on the overview of the roles of the various crystalline planes, it is evident that constructing electrocatalysts with synergistic multiple crystalline planes is more favourable for NO_x^- reduction.[68] For example, the Cu nanosheets benefit from the tandem interactions between the Cu(100) and Cu (111) facets, obtaining an excellent NH_3 yield of 1.41 mmol h^{-1} cm^{-2} and remarkable stability reaching 700 h at −0.59 V. As depicted in Fig. 6c, NO_2^- formed on the Cu(100) surface is subsequently hydrogenated on the Cu(111) surface; such tandem catalysis accelerates the hydrogenation of *NO to *NOH and the generation of NH_3.[69]

Meanwhile, defects have been proved to promote NO_x^- reduction processes in synergy with diverse crystal planes. Ultrathin copper oxide nanoribbons are obtained by *in situ* electrochemical reduction with exposed Cu(100) surfaces and abundant surface defects, achieving 2.3 times higher NH_3 yield in the NO_3^- reduction process than that *via* the Haber–Bosch process. The key to their outstanding property is the upshifting of the Cu d-band center due to the synergistic effect of the Cu(100) facets and defects; this facilitates the increased adsorption intensities of $*NO_3$ and *H, thus reducing the NO_3^- reduction potential and inhibiting the HER.[70] The contributions of surface oxygen species (oxygen vacancies and hydroxyl groups) on Cu_2O have also been demonstrated to promote NO_3^- reduction. Chen's group obtained Cu_2O(111) surfaces with more oxygen vacancies and hydroxyl groups than the Cu_2O(100) facets.[71] It was also confirmed that the adsorption of reactants and intermediates was accelerated by oxygen vacancies on the Cu_2O(111) surfaces, while the HER competition could be inhibited by surface hydroxyl groups (Fig. 6d).

Exposing specific facets can effectively enhance the activity of Cu-based catalysts, but the robustness of the material falls far short of expectations. The pure Cu catalysts are rapidly deactivated during NO_x^- reduction by poisoning from adsorbed nitrogenous species and hydrogen, with current densities attenuating by over half in six minutes under potentials exceeding −0.5 V.[72] Gao *et al.* proposed a strategy of pulsed electrolysis of Cu to obtain Cu/Cu_2O through peroxidation and self-repair processes,[73] and the Cu/Cu_2O catalysts obtained by pulsed electrolysis were more favourable for both NO_3^- and NO_2^- reduction processes than the static electroreduction on Cu. However, the accumulation of NO_2^- during NO_3^- reduction is still not ignored; this is attributed to the excessively aggressive HER competition hampering subsequent hydrogenation processes. The regulated pH and enhanced cathodic potential naturally facilitate the hydrogenation process to a certain extent, but the degree of enhancement is inadequate. Consequently, pulsed electrolysis of CuNi alloy is employed to introduce $Ni(OH)_2$ promoting H intermediate formation, which contributes to the improvement of the H adsorption capacity (Fig. 7a). The tandem catalysis of Cu-based and Ni-based materials breaks the awkward scenario (Fig. 7b) of the simultaneous existence of rapid NO_3^- transformation to NO_2^- (reaction (1)) and sluggish subsequent hydrogenation (reaction (2)), enabling a more efficient and stable catalytic NO_3^- reduction process at lower potentials.

In addition to the cathode potential and pH, CO_2 has also been confirmed to affect the NO_2^- reduction process on copper catalysts. Sun's group demonstrated that the faradaic efficiencies of copper catalysts could reach approximately

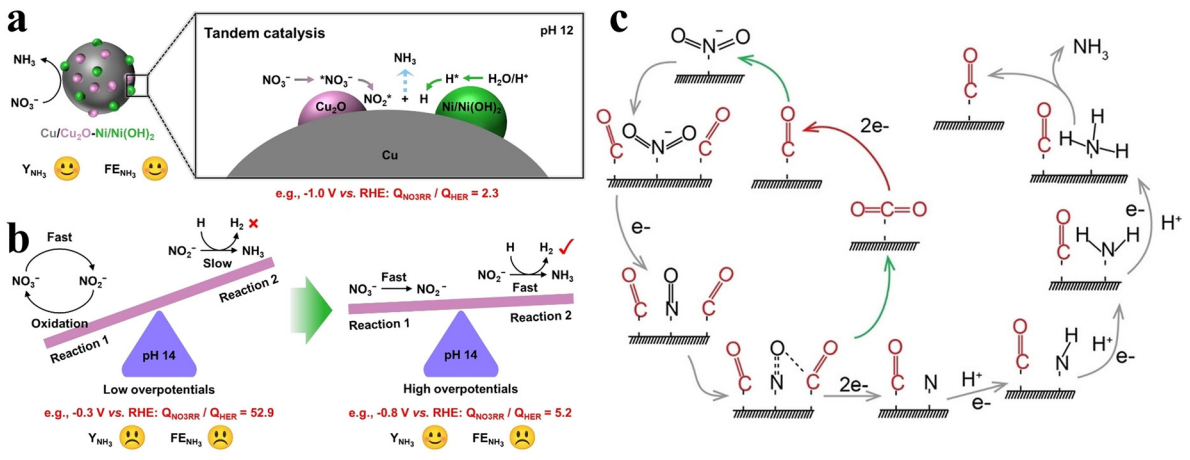

Fig. 7 (a) Tandem catalysis of CuNi alloy under pulsed electrolysis. (b) Kinetic regulation process of NO_3^- reduction copied with permission.[73] Copyright 2023, John Wiley and Sons. (c) NO_2^- reduction reaction pathway assisted by CO_2 copied with permission.[74] Copyright 2022, John Wiley and Sons.

100% for NO_2^- reduction within a wide range of potentials assisted by CO_2.[74] The causes of the enhanced performance due to CO_2 are described in Fig. 7c. The *CO species obtained from CO_2 reduction simultaneously facilitate deoxygenation of the *NO intermediates and hydrogenation of the *NH_2 intermediate in the NO_2^- reduction process. In the facilitated *NO conversion process to *N, *CO is oxidized to CO_2 by *NO. CO_2 assisted strategies also prove to be beneficial for nitrate electroreduction.

3.3. Fe-based electrocatalysts

In nature, anammox bacteria have been proved to exploit Fe^0/Fe^{2+} as electron donors for the denitrification of NO_3^- and NO_2^-.[75] In addition, the presence of Fe as the active site in nitrogenase enzymes has also promoted considerable exploration of Fe-based electrocatalysts with abundance on Earth.[44] The performances of currently developed Fe-based electrocatalysts are listed in Table 2. Recently, a deeper understanding has emerged of the intrinsic catalytic behavior on Fe isolated sites for NO_x^- reduction. The nitrogen-coordinated Fe single atoms on carbon were obtained *via* a polymer-hydrogel strategy.[76] The turnover frequency of synthesized Fe single sites is 12 times larger than that of metallic Fe nanoparticles. DFT calculations confirm that the NO_3^--preemption mechanism may occur in the catalytic process for Fe single atoms, effectively preventing strong water adsorption. Despite extensive studies on single-atom catalysts, which maximize the utilization of active atoms, the performance of single-atom catalysts is still limited in the multi-step NO_x^- reduction process due to the intrinsic adsorption energy scaling relationship. Dual-atom catalysts exhibit more favourable performance in multi-step reactions compared with single-atom catalysts, which inherit the advantages of single-atom catalysts and possess the synergistic effect of two sites.[77] For example, FeMo@g-CN has been theoretically proved to exhibit a promising limiting potential (−0.34 V) for forming NH_3 through NO_3^- reduction.[78] The activation of NO_3^- reduction in FeMo@g-CN is verified to originate from the synergistic interaction of FeMo dimer d orbitals rather than specific d suborbitals.

In addition to Fe single-atom catalysts, oxides of iron have received considerable attention. Wang *et al.* synthesized Fe_3O_4 doped with appropriate amounts of Cu,[79] achieving an ammonia yield of 222.75 ± 12.15 mg h^{-1} mg_{cat}^{-1} and an excellent FE of 95.7% ± 4.8 at −0.7 V. More intriguingly, in addition to enhancing the adsorption of various intermediates (Fig. 8a), the doping of Cu alters the state of *NO adsorbed on the metal

Table 2 Summary of NO_x^- reduction performance of Fe-based electrocatalysts

Electrocatalyst	Electrolyte	Potential (V *vs.* RHE)	NH_3 yield	Faradaic efficiency (%)	Ref.
Fe–PPy SACs	0.1 M KOH + 0.1 M NO_3^-	−0.2	2.75 mg h^{-1} cm^{-2}	100	76
Cu–Fe_3O_4	0.1 M KOH + 0.1 M KNO_3	−0.6	179.55 mg h^{-1} mg_{cat}^{-1}	100	79
Fe–cyano NSs	1.0 M KOH + 10 mM KNO_3	−0.5	42.1 mg h^{-1} mg_{cat}^{-1}	90	49
P–$FeCo_2O_4$@CC	0.1 M KOH + 0.1 M KNO_2	−0.4	5.29 mg h^{-1} cm^{-2}	99.99	111
FeP	0.1 M KOH + 0.1 M KNO_2	−0.5 V	—	85	112

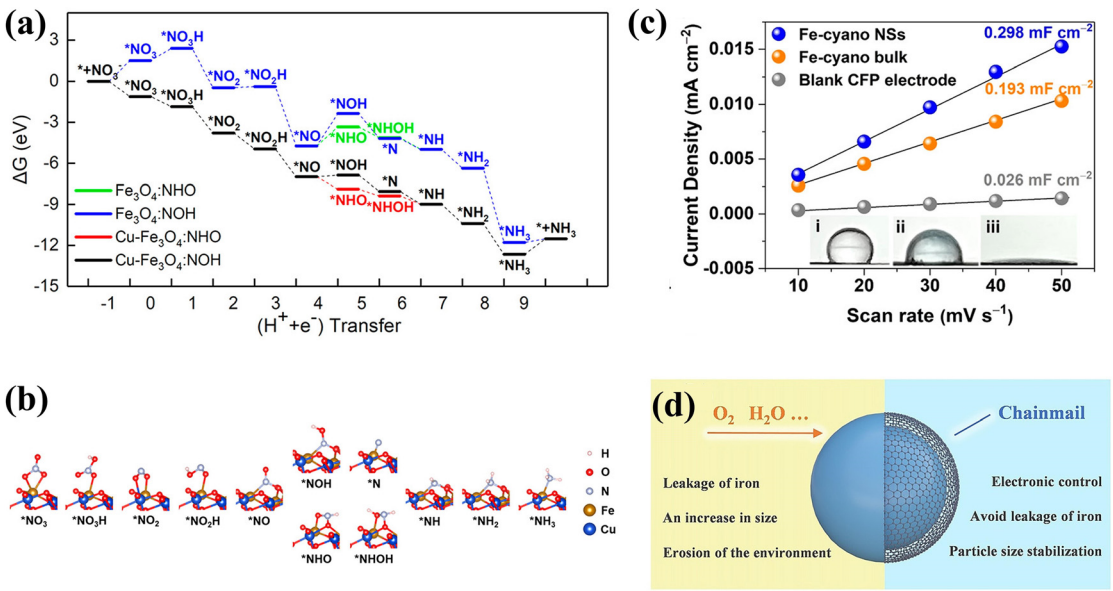

Fig. 8 (a) Gibbs free energy plot of NO_3^- reduction on the electrocatalyst surfaces. (b) Optimized structures of the intermediates on the Cu-doped Fe_3O_4 surface during NO_3^- reduction copied with permission.[79] Copyright 2023, American Chemical Society. (c) ECSA and contact angles of different catalysts copied with permission.[49] Copyright 2021, American Chemical Society. (d) Schematic diagram of the action of graphene armour copied with permission.[80] Copyright 2022, John Wiley and Sons.

atoms. *NO is susceptible to reaction poisoning due to strong adsorption. The *NO in Fe_3O_4 is adsorbed vertically on the Fe atom. After Cu doping, *NO adsorption is carried out by the bridge between Fe and O atoms, thus *NO preferentially undergoes the route of reduction to *NHO rather than the route to *NOH with higher ΔG (Fig. 8b).

Indeed, the hydrophilicity of materials is also worth considering, and hydrophilic materials are more conducive to the adsorption of NO_x^- ions. However, the hydrophobic surface of the bulk metal catalyst inhibits mass transport and diminishes the overall electrochemical surface area due to the dramatically reduced contact of the electrocatalyst with the electrolyte. Metallocyano polymers are a class of superhydrophilic materials suitable for efficient electrocatalysis due to the abundance of hydrophilic groups and surface vacancies. The Fe–cyano NSs with a two-dimensional structure display a high NH_3 yield reaching 42.1 mg h^{-1} mg_{cat}^{-1} and FE exceeding 90% at −0.5 V *vs.* RHE.[49] Furthermore, an electrolyzer based on Fe–cyano NSs as the cathode and anode has been constructed with an energy efficiency of 26.2%. As illustrated in Fig. 8c, Fe–cyano NSs possess a superhydrophilic surface and distinctly larger active area owing to the nature of the cyano groups and two-dimensional structure, which facilitates enhanced molecular adsorption and provides speedier transport avenues for electrolyte diffusion and electron transport.

The Fe-based catalysts exhibit decent nitrate reduction activity, but the catalysts still suffer from the limitations of inferior long-term robustness and poor kinetic durability in the practical catalytic process.[20] The recent exploitation of chainmail-protected catalysts has offered innovative insights into the design of high-efficiency and robust Fe-based catalysts. Fe nanoparticles suffer from poor durability due to their greater susceptibility to leaching and oxidation during the electrocatalytic process. Zhang *et al.* prepared Fe nanoparticles protected by ultrathin graphene nanosheet layers (Fe@Gnc) for NO_3^- conversion to N_2; the NO_3^- conversion rate and N_2 selectivity of Fe@Gnc remained in excess of 96% after 960 hours of cycling.[80] The contribution of graphene nanochainmail is depicted in Fig. 8d. In the absence of graphene nanochainmail protection, active site agglomeration and toxic inactivation would occur on Fe particles. With the protection of graphene nanochainmail, the aggregation issue is not only tackled, but electron/ion transport is also accelerated by favorably conducting graphene for highly efficient and more sustained NO_3^- conversion. Despite the fact that Fe@Gnc is employed for NO_3^- reduction to N_2, it is still valid to draw inspiration from the construction of Fe@Gnc for NH_3 production. Substituting the sites requiring protection for other high NH_3 selectivity sites might be a promising strategy.

3.4. Co-based electrocatalysts

Co has attracted extensive interest due to its low activation energy barriers for dissociating intermediates such as $*NO_3$, $*NO_2$, *NO and $*N_2O$.[81] The Co based materials in Table 3 all show decent performances. Recently, the Gibbs free energies (ΔG_{rxn}) of the associated rate-determined step were compared for NO_3^- reduction on commonly available metals through theoretical screening. As shown in Fig. 9a and b, ΔG_{rxn} of the rate-determining step on Co exhibits the lowest value of 0.3 V.[82] Furthermore, Shao *et al.* demonstrated through DFT calculations that surface oxygen on Co sites could stabilize hydrogen adsorbed on the Co oxides, thus inhibiting the HER and causing enhanced activity of electrocatalytic NO_x^- reduction to NH_3.[83] Consequently, Co and Co oxides have also received considerable attention for nitrate reduction in recent years.[84] Hybrid nanoparticles of metallic Co and Co oxides containing Co, Co^{2+} and Co^{3+} were prepared by a simple electrodeposition strategy and the catalysts exhibited excellent NO_x^- reduction performance (FE: 100% at −0.2 V) and OER activity (η_{10} = 310 mV).[82] A zinc nitrate cell assembled from the catalysts demonstrated an outstanding power density of 25 mW cm^{-2}.

Cobalt phosphide has also been probed extensively for NO_x^- reduction.[85] The introduction of P has been confirmed to improve the stability of the catalysts by mitigating the reconstitution of Co to form $Co(OH)_2$ during NO_3^- reduction, while reducing ΔG_{rxn} of the rate-determining step and optimizing the required energy barriers for the reaction. In addition, the Co 4p orbitals in CoP proved to be engaged directly in the NO_3^- adsorption and electron transfer steps. The mechanism of CoP action in NO_3^- reduction is shown in Fig. 9c. Initially, empty Co 4p orbitals in CoP are coupled with O 2p orbitals in NO_3^- to form the Co–O–N bond for NO_3^- adsorption on Co sites. With the employment of a strong electrical field, the Co 4p orbitals obtain excited electrons from the Co 3d orbitals. Subsequently, electrons in the Co 4p orbitals are shifted to O 2p orbitals *via* the Co–O–N covalent bond and infused into the π* orbitals of NO_3^-, causing considerably reduced NO_3^- adsorption for accelerated reduction to NH_3. The CoP nanoarrays also exhibit promising performance in the NO_2^- electroreduction process, reaching a NH_3 yield of 2260.7 ± 51.5 μg h^{-1} cm^{-2} and a FE of 90.0 ± 2.3% at −0.2 V *vs.* RHE.[86] DFT calculations have confirmed the dominance of NO_2^- electroreduc-

Table 3 Summary of NO_x^- reduction performance of Co-based electrocatalysts

Electrocatalyst	Electrolyte	Potential (V *vs.* RHE)	NH_3 yield	Faradaic efficiency (%)	Ref.
DM–Co	1 M KOH + 1 M KNO_3	−0.2	1.2 mmol h^{-1} cm^{-2}	100	82
CoOx	0.1 M KOH + 0.1 M KNO_3	−0.5	82.4 mg h^{-1} mg_{cat}^{-1}	93.4	83
CoP NAs/CFC	1.0 M NaOH + 1.0 M $NaNO_3$	−0.3	9.56 mol h^{-1} m^{-2}	100	85
Ru_xCo_y alloy	0.1 M KOH + 0.1 M KNO_3	0	3.21 mol g_{cat}^{-1} h^{-1}	97	87
C/Co_3O_4	50 mM K_2SO_4 + 50 mM KNO_2	−0.6	4.1 mg h^{-1} cm^{-2}	100	12
CoP NA/TM	0.1 M PBS + 500 ppm NO_2^-	−0.2	2,26 mg h^{-1} cm^{-2}	90	86

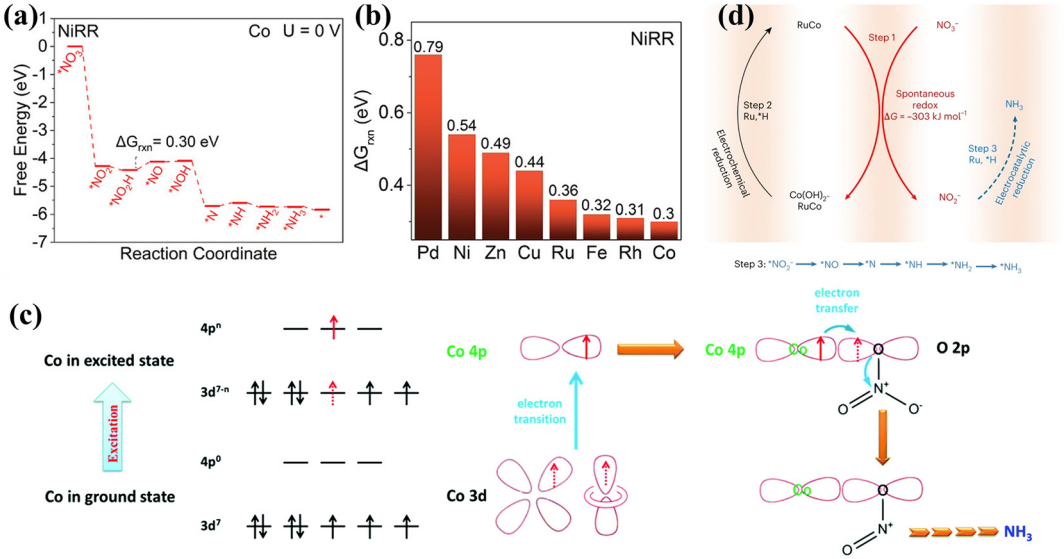

Fig. 9 (a) The Gibbs energy diagram of NO_3^- reduction on the Co surface. (b) ΔG_{rxn} on different metals copied with permission.[82] Copyright 2022, John Wiley and Sons. (c) Mechanism of NO_3^- reduction on CoP copied with permission.[85] Copyright 2022, Royal Society of Chemistry. (d) The three-step relay route of Ru_xCo_y alloy copied with permission.[87] Copyright 2023, Springer Nature.

tion over the HER, owing to the much smaller adsorption energy (−0.6 eV) of NO_2^- on CoP(112) compared to that of H (−0.12 eV).

The doping of P can suppress the reconstruction of Co, while the introduction of Ru can achieve the reconversion of $Co(OH)_2$ to Co for more efficient and durable ammonia production.[87] Co and NO_3^- are spontaneously converted to form Co $(OH)_2$ and NO_2^-, and the conversion of $Co(OH)_2$ to Co and NO_2^- reduction to NH_3 can be facilitated by active hydrogen species. In view of Ru having decent adsorption energies for hydrogen atoms, Ru_xCo_y alloy hollow nanostructures have been developed to achieve NH_3 production with a remarkable energy efficiency of 42 ± 2%. As indicated in Fig. 9d, the existence of Ru facilitates the formation of active hydrogen species, promoting a dynamic Co valence cycle and achieving an innovative three-step relay route involving spontaneous redox reactions, electrochemical reduction and electrocatalytic reduction.

3.5. Ni-based and Ti-based electrocatalysts

Aiming to eliminate competition from the HER in NO_x^- reduction, scientists have generally been drawn to metals that are relatively inert in the water splitting process, like Cu.[88] However, the hydrogenation process of NO_x^- reduction is also urgently required for the generation of H* *via* water splitting. HER-active metals including Ni can facilitate significant H* generation,[89–91] which can also be promising catalysts for ammonia production after effectively obviating the direct coupling path of H*. The Ni based materials in Table 4 also show promising performance. For example, the self-activated Ni $(OH)_2$@Ni cathode was tested on a pilot scale for the treatment of wastewater containing nitrate (Fig. 10a) showing no decay in the reaction rate after two months of successive operation (Fig. 10b).[92] The impressive properties of $Ni(OH)_2$@Ni are conjectured to stem from inhibiting the HER in the H*-mediated NO_3^- reduction pathway, thus promoting the reduction of NO_3^- to NH_3.

The construction of grain boundary defect engineering on nickel nanoparticles (GB Ni-NPs) is also well-suited to simultaneously achieving the availability of sufficient H* and suppressing competition from the HER.[93] As illustrated in Fig. 10c and d, the increased H* retention potential results from the GB region having a higher energy barrier for H_2 formation from H*. Compared with pristine Ni, abundant H* in GB Ni-NPs is inclined to combine with adjacent adsorbed intermediates for NH_3 production, rather than coupling directly to produce H_2. Furthermore, the appropriate adsorption energies of GB Ni-NPs for key species (Fig. 10e) facilitate the conversion of NO_3* to NO_2* and accelerate the dissociation of NH_3.

Table 4 Summary of NO_x^- reduction performance of Ni-based electrocatalysts

Electrocatalyst	Electrolyte	Potential (V *vs.* RHE)	NH_3 yield	Faradaic efficiency (%)	Ref.
$Ni(OH)_2$@Ni	0.1 M Na_2SO_4 + 70 mg L^{-1} NO_3^-	3.67	—	95.5	92
GB Ni-NPs	1 M NaOH + 1 M $NaNO_3$	−0.93	15.49 mmol h^{-1} cm^{-2}	90	93
Ni–TiO_2	0.1 M NaOH + 0.1 M NO_2^-	−0.7	727 μmol h^{-1} cm^{-2}	90	94
Ni@JBC	0.1 M NaOH + 0.1 M NO_2^-	−0.5	4.1 mg h^{-1} mg_{cat}^{-1}	83.4	113
Ni-NSA-VN	50 mM K_2SO_4 + 50 mM KNO_2	−0.6	—	95.5	114

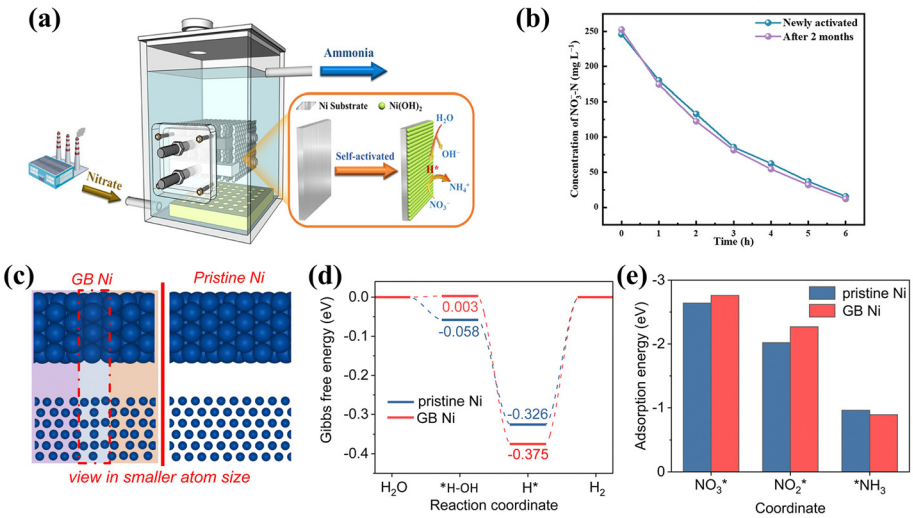

Fig. 10 (a) Diagram of an electrochemical reactor on the pilot scale and (b) comparison of initial NO_3^- reduction performance and that after two months copied with permission.[92] Copyright 2021, American Chemical Society. (c) The simulated structure, (d) Gibbs free energy diagrams of the HER and (e) adsorption energies of important N-containing species on GB Ni and pristine Ni copied with permission.[93] Copyright 2023, Royal Society of Chemistry.

For the design of NO_x^- reduction catalysts, facilitating the hydrogenation process of the intermediate is essential, and the enhanced adsorption of NO_x^- should also not be neglected. The introduction of Ni into TiO_2 can significantly boost the nitrite reduction performance of TiO_2.[94] The improved material has an excellent FE as high as 94.89% at −0.5 V and a maximum NH_3 yield reaching 727 μmol h^{-1} cm^{-2} at −0.7 V. Theoretical calculations have confirmed that the introduction of Ni lowers the energy barrier in the critical conversion step of *NO to *N, thus enhancing the adsorption of NO_2^- and promoting the conversion of NO_2^- to NH_3.

TiO_2 is the most broadly studied Ti-based material due to its high abundance, low cost, non-toxicity and excellent stability, nevertheless it also encounters deficiencies such as poor electrical conductivity and insufficient active sites.[95,96] A variety of strategies including vacancy engineering,[97] introducing metal atoms[98] and non-metal atom doping[96] have been employed to modify TiO_2; these have achieved positive results (Table 5). More interestingly, TiO_2 is also a typical n-type semiconductor with significant chemical and structural stability,[99] which can be employed for the construction of Mott–Schottky junctions and p–n heterojunctions.

It is often perceived that two oppositely charged regions across the interface can be created by the construction of a semiconductor junction, along with a strong built-in field, which can modify the atomic interfacial electron density.[100] Mott–Schottky junctions can be formed by combining conductors (metals) with semiconducting materials. Accelerated electronic transfers at the interface and strong built-in electric field formation can be induced by discrepancies in the Fermi energy levels between metals and semiconductors, promoting local charge polarization and significantly ameliorating the adsorption of key intermediates.[101]

Co@TiO_2 heterostructures exhibit superior NO_3^- reduction performance due to the Schottky interface.[102] The effects of the Schottky junction are mainly manifested in the enhanced electronic conductivity and the improved catalytic selectivity. The mapping of the electron density difference (Fig. 11a) in Co@TiO_2 also confirms electron migration from the Co side to the TiO_2 side, resulting in electron depletion regions on the Co surface. The built-in electric field can be generated due to the accumulation of net charge on the TiO_2 side, promoting the transportation of charge. DFT calculations (Fig. 11b) have also revealed that the Schottky junction of Co@TiO_2 indeed promotes NO_3^- adsorption and inhibits the appearance of by-products including NO_2, NO, and N_2.

The p–n junction can also be formed by coupling TiO_2 with a p-type semiconductor, thus inducing charge redistribution

Table 5 Summary of NO_x^- reduction performance of Ti-based electrocatalysts

Electrocatalyst	Electrolyte	Potential (V *vs.* RHE)	NH_3 yield	Faradaic efficiency (%)	Ref.
CoP/TiO_2@TP	0.1 M NaOH + 0.1 M $NaNO_3$	−0.5	499.8 μmol h^{-1} cm^{-2}	95	103
Co@TiO_2/TP	0.1 M PBS + 0.1 M NO_3^-	−0.93	800 μmol h^{-1} cm^{-2}	96.7	102
Cu–TiO_2	0.1 M Na_2SO_4 + 0.1 M NO_3^-	−0.3	—	84.3	115
TiO_{2-x}	0.5 M Na_2SO_4 + 0.5 M NO_3^-	−0.4	—	85	40
Cu_3P@TiO_2/TP	0.1 M NaOH + 0.1 M $NaNO_2$	−0.7	1583.4 μmol h^{-1} cm^{-2}	97.1	116
V–TiO_2	0.1 M NaOH + 0.1 M NO_2^-	−0.7	540.8 μmol h^{-1} cm^{-2}	93.2	98

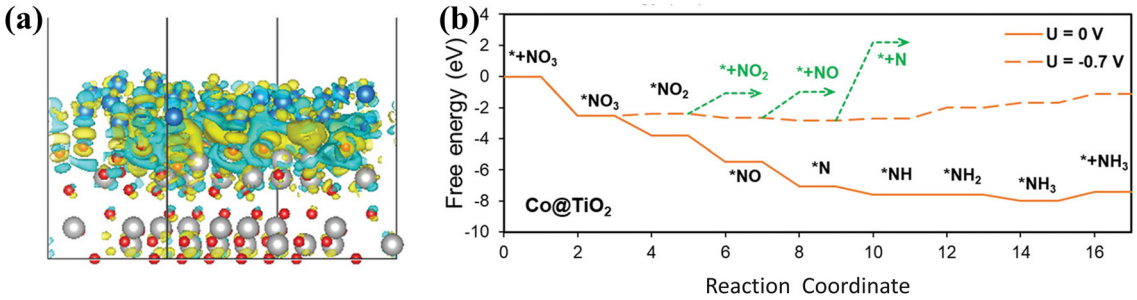

Fig. 11 (a) Mapping of the electron density difference. (b) Free energy diagram for NO_3^- conversion on Co@TiO_2 copied with permission.[102] Copyright 2023, John Wiley and Sons.

in the material and optimising the adsorption free energies of the intermediates. The p–n junction of CoP/TiO_2 heterostructures has been confirmed by experimental and theoretical studies to achieve a lower energy barrier of NO_3^- conversion to $*NO_3^-$ and increased energy barriers of NO and NO_2 production, which enhance the NO_3^- reduction activity and optimise the reaction selectivity.[103]

In summary, a variety of strategies for optimizing transition metal-based catalysts have been demonstrated. Alloying and doping are common tactics to modulate the d-band center and intermediate adsorption energies of metals, but it is important to select inexpensive elements to effectively assist transition metals at accelerating NO_x^- reduction. Exposure of specific crystalline surfaces and vacancy engineering are also effective optimization strategies to effectively boost reactant and intermediate adsorption, but obtained materials show limited activity enhancement with undesired stability. The construction of heterostructures can dramatically enhance catalytic activity and selectivity caused by their intriguing physical nature due to redistributed charges and bent energy bands at the heterogeneous interface. The key to constructing superior heterostructures is the selection of coupling materials. The design of chainmail-protected catalysts offers novel insights to significantly improve catalyst stability, but the selection of suitable materials as chainmail and the exploration of gentle synthesis strategies require more attention. In addition to the optimization strategies mentioned above, other factors such as atmosphere and anions in the electrolyte may also considerably contribute to the catalytic activity and selectivity of materials, however, there are few systematic and insightful studies on the contributions of other factors to accelerate NO_x^- reduction.

4. Conclusion and future outlook

Electrocatalytic NO_x^- reduction provides innovative insights into sustainable NH_3 synthesis and eco-friendly NO_x^- removal. The review firstly outlines the mechanism of NO_x^- reduction and the challenges of catalyst design under aqueous conditions, proposing that the following points should be observed when designing electrocatalysts with excellent performance: (1) The adsorptions of NO_3^- and NO_2^- on catalysts are vital. For NO_3^- reduction, the conversion from NO_3^- to NO_2^- is a decisive step. Suitable adsorptions of NO_3^- and NO_2^- are beneficial for the reaction. (2) It is difficult to escape competition with the HER under aqueous conditions. Suppressing the formation of active hydrogen species is unadvisable to reduce HER competition because active hydrogen species are indispensable reactants for the subsequent hydrogenation process in NO_x^- reduction. The strategy of employing two sites can be used for reference to simultaneously realize active hydrogen species production and reduce the direct coupling of active hydrogen species. In this strategy, one site acts as a proton warehouse to promote proton generation, and the other site temporarily stores active hydrogen species for subsequent hydrogenation reactions. (3) In addition to the HER side reaction, other side reactions generating N_2 or NO should not be ignored. Improved stability of intermediates including $*NO_2$ or *NOH facilitates more efficient ammonia production.

Then, this paper focuses on widely studied first-row transition metal-based electrocatalysts including Cu, Fe, Co, Ni, Ti-based electrocatalysts, which are characterized by tempting abundance and moderate interactions with the reactants. Recent advances in engineering first-row transition metal-based electrocatalysts are presented in this paper. Hopefully these provide more inspiration for constructing remarkable NO_x^- reduction electrocatalysts. Despite the tremendous advances that have been obtained in currently developed catalysts, a series of challenges still exist in this area and are waiting to be addressed:

(i) Currently, in the field of NO_x^- reduction, the lack of benchmark catalysts makes it difficult to measure the gap between the experimentally prepared materials and industrialization. In addition, the use of isotope labeling to verify the effective transformation of NO_x^- is questionable and lacks standardization in current experiments. Researchers often choose isotopes with low purity in practical experiments, considering that isotopes with high purity will bring excessive experimental cost. Meanwhile, isotope labeling with low purity makes it difficult to exclude the interference of other N species including N_2.

(ii) Inconsistent descriptions of ammonia production units such as mg h^{-1} cm^{-2} and mmol h^{-1} mg_{cat}^{-1} are employed in current articles, which is unfavourable for readers and peers to

judge the performance level of materials. Employing uniform units is more conducive to accelerating the development of NO_x^- electrocatalysts.

(iii) It is common for catalysts to undergo reconfiguration during the catalytic process, but the reconfiguration problem is rarely explored in currently developed NO_x^- reduction electrocatalysts; more advanced characterization techniques are required to be employed in the study of catalytic mechanisms.

(iv) The oxygen evolution reaction (OER) is usually employed as the anode reaction in aqueous catalytic installations for NO_x^- reduction to NH_3. Replacing the OER with other reactions including Zn oxidation or methanol oxidation can result in more value-added product synthesis or the Zn–NO_x^- cell simultaneously producing NH_3 and electricity. These intriguing replacements can open up novel insights into the diverse applications of NO_x^- reduction.

(v) In addition to the development of catalysts with superior performance, electricity prices are also worth considering for promoting the realization of large-scale electrocatalytic NO_x^- reduction to NH_3. Much lower electricity prices may come with the development of alternative energy sources such as plasma and nuclear fusion.

(vi) A stable NO_x^- source has long been a topic of concern. It is necessary to consider the complex composition of wastewater employed as a source. Several studies have confirmed the significant influences of ion concentration, other inorganic ions, and pH on nitrate reduction in wastewater.

(vii) When selecting wastewater as source of NO_x^- ions, complex composition of wastewater should be considered. Other ions and pH interference cannot be ignored, from the current situation, the cost of enrichment wastewater is also necessary to consider. Direct synthesis through electrocatalytic nitrogen oxidation also faces the challenge of developing highly active nitrogen oxidation catalysts.

(viii) Although the majority of catalysts currently developed exhibit decent stability, most of them are tested at the experimental scale. It is necessary to carry out stability tests on catalysts at the pilot scale or larger scale.

Conflicts of interest

There are no conflicts of interest to declare.

Acknowledgements

This work was supported by the National Natural Science Foundation of China (Grant No. 22179065).

References

1 W. Chen, X. Yang, Z. Chen, Z. Ou, J. Hu, Y. Xu, Y. Li, X. Ren, S. Ye, J. Qiu, J. Liu and Q. Zhang, Emerging applications, developments, prospects, and challenges of electrochemical nitrate-to-ammonia conversion, *Adv. Funct. Mater.*, 2023, 2300512, DOI: **10.1002/adfm.202300512**.

2 Y. Wang, C. Wang, M. Li, Y. Yu and B. Zhang, Nitrate electroreduction: mechanism insight, in situ characterization, performance evaluation, and challenges, *Chem. Soc. Rev.*, 2021, **50**, 6720–6733, DOI: **10.1039/D1CS00116G**.

3 D. Ye and S. C. E. Tsang, Prospects and challenges of green ammonia synthesis, *Nat. Synth.*, 2023, **2**, 612–623, DOI: **10.1038/s44160-023-00321-7**.

4 B. Lee, L. R. Winter, H. Lee, D. Lim, H. Lim and M. Elimelech, Pathways to a green ammonia future, *ACS Energy Lett.*, 2022, **7**, 3032–3038, DOI: **10.1021/acsenergylett.2c01615**.

5 J. Lim, C. A. Fernández, S. W. Lee and M. C. Hatzell, Ammonia and nitric acid demands for fertilizer use in 2050, *ACS Energy Lett.*, 2021, **6**, 3676–3685, DOI: **10.1021/acsenergylett.1c01614**.

6 C. Smith, A. K. Hill and L. Torrente-Murciano, Current and future role of haber bosch ammonia in a carbon-free energy landscape, *Energy Environ. Sci.*, 2020, **13**, 331–344, DOI: **10.1039/C9EE02873K**.

7 X. Fu, J. Zhang and Y. Kang, Recent advances and challenges of electrochemical ammonia synthesis, *Chem. Catal.*, 2022, **2**, 2590–2613, DOI: **10.1016/j.checat.2022.09.001**.

8 X. Lv, C. Weng and Z. Yuan, Ambient ammonia electrosynthesis: current status, challenges, and perspectives, *ChemSusChem*, 2020, **13**, 3061–3078, DOI: **10.1002/cssc.202000670**.

9 D. Liu, L. Qiao, S. Peng, H. Bai, C. Liu, W. F. Ip, K. H. Lo, H. Liu, K. W. Ng, S. Wang, X. Yang and H. Pan, Recent advances in electrocatalysts for efficient nitrate reduction to ammonia, *Adv. Funct. Mater.*, 2023, 2303480, DOI: **10.1002/adfm.202303480**.

10 X. Lv, X. Liu, Y. Suo, Y. Liu and Z. Yuan, Identifying the dominant role of pyridinic-N-Mo bonding in synergistic electrocatalysis for ambient nitrogen reduction, *ACS Nano*, 2021, **15**, 12109–12118, DOI: **10.1021/acsnano.1c03465**.

11 J. Choi, B. H. R. Suryanto, D. Wang, H. Du, R. Y. Hodgetts, F. M. Ferrero Vallana, D. R. Macfarlane and A. N. Simonov, Identification and elimination of false positives in electrochemical nitrogen reduction studies, *Nat. Commun.*, 2020, **11**, 5546, DOI: **10.1038/s41467-020-19130-z**.

12 R. Zhang, S. Zhang, Y. Guo, C. Li, J. Liu, Z. Huang, Y. Zhao, Y. Li and C. Zhi, A Zn-nitrite battery as an energy-output electrocatalytic system for high-efficiency ammonia synthesis using carbon-doped cobalt oxide nanotubes, *Energy Environ. Sci.*, 2022, **15**, 3024–3032, DOI: **10.1039/D2EE00686C**.

13 J. Li, G. Zhan, J. Yang, F. Quan, C. Mao, Y. Liu, B. Wang, F. Lei, L. Li, A. W. M. Chan, L. Xu, Y. Shi, Y. Du, W. Hao, P. K. Wong, J. Wang, S. Dou, L. Zhang and J. C. Yu, Efficient ammonia electrosynthesis from nitrate on strained ruthenium nanoclusters, *J. Am. Chem. Soc.*, 2020, **142**, 7036–7046, DOI: **10.1021/jacs.0c00418**.

14 S. Meng, C. Zhang, C. Ye, J. Li, S. Zhou, L. Zhu, X. Li, C. Tung and L. Wu, Cobaloximes: selective nitrite reduction catalysts for tandem ammonia synthesis, *Energy Environ. Sci.*, 2023, **16**, 1590–1596, DOI: 10.1039/D2EE03956G.

15 N. Zhang, J. Shang, X. Deng, L. Cai, R. Long, Y. Xiong and Y. Chai, Governing interlayer strain in bismuth nanocrystals for efficient ammonia electrosynthesis from nitrate reduction, *ACS Nano*, 2022, **16**, 4795–4804, DOI: 10.1021/acsnano.2c00101.

16 P. H. van Langevelde, I. Katsounaros and M. T. M. Koper, Electrocatalytic nitrate reduction for sustainable ammonia production, *Joule*, 2021, **5**, 290–294, DOI: 10.1016/j.joule.2020.12.025.

17 S. Liu, M. Wang, Q. Cheng, Y. He, J. Ni, J. Liu, C. Yan and T. Qian, Turning waste into wealth: sustainable production of high-value-added chemicals from catalytic coupling of carbon dioxide and nitrogenous small molecules, *ACS Nano*, 2022, **16**, 17911–17930, DOI: 10.1021/acsnano.2c09168.

18 S. Yeon, S. J. Lee, J. Kim, T. Begildayeva, A. Min, J. Theerthagiri, M. L. A. Kumari, L. M. C. Pinto, H. Kong and M. Y. Choi, Sustainable removal of nitrite waste to value-added ammonia on Cu@Cu_2O core–shell nanostructures by pulsed laser technique, *Environ. Res.*, 2022, **215**, 114154, DOI: 10.1016/j.envres.2022.114154.

19 X. Deng, Y. Yang, L. Wang, X. Fu and J. Luo, Metallic Co nanoarray catalyzes selective NH_3 production from electrochemical nitrate reduction at current densities exceeding 2 A cm^{-2}, *Adv. Sci.*, 2021, **8**, 2004523, DOI: 10.1002/advs.202004523.

20 C. Fu, S. Shu, L. Hu, Z. Liu, Z. Yin, X. Lv, S. Zhang and G. Jiang, Electrocatalytic nitrate reduction on bimetallic palladium-copper nanowires: key surface structure for selective dinitrogen formation, *Chem. Eng. J.*, 2022, **435**, 134969, DOI: 10.1016/j.cej.2022.134969.

21 X. Zou, J. Xie, C. Wang, G. Jiang, K. Tang and C. Chen, Electrochemical nitrate reduction to produce ammonia integrated into wastewater treatment: investigations and challenges, *Chin. Chem. Lett.*, 2023, **34**, 107908, DOI: 10.1016/j.cclet.2022.107908.

22 J. G. Chen, R. M. Crooks, L. C. Seefeldt, K. L. Bren, R. M. Bullock, M. Y. Darensbourg, P. L. Holland, B. Hoffman, M. J. Janik and A. K. Jones, Beyond fossil fuel driven nitrogen transformations, *Science*, 2018, **360**, eaar6611, DOI: 10.1126/science.aar6611.

23 L. Zhang, M. Cong, X. Ding, Y. Jin, F. Xu, Y. Wang, L. Chen and L. Zhang, A janus Fe-SnO_2 catalyst that enables bifunctional electrochemical nitrogen fixation, *Angew. Chem., Int. Ed.*, 2020, **59**, 10888–10893, DOI: 10.1002/anie.202003518.

24 T. Li, S. Han, C. Wang, Y. Huang, Y. Wang, Y. Yu and B. Zhang, Ru-doped Pd nanoparticles for nitrogen electrooxidation to nitrate, *ACS Catal.*, 2021, **11**, 14032–14037, DOI: 10.1021/acscatal.1c04360.

25 M. Anand, C. S. Abraham and J. K. Nørskov, Electrochemical oxidation of molecular nitrogen to nitric acid towards a molecular level understanding of the challenges, *Chem. Sci.*, 2021, **12**, 6442–6448, DOI: 10.1039/D1SC00752A.

26 J. Liu, D. Richards, N. Singh and B. R. Goldsmith, Activity and selectivity trends in electrocatalytic nitrate reduction on transition metals, *ACS Catal.*, 2019, **9**, 7052–7064, DOI: 10.1021/acscatal.9b02179.

27 H. Xu, Y. Ma, J. Chen, W. X. Zhang and J. Yang, Electrocatalytic reduction of nitrate: a step towards a sustainable nitrogen cycle, *Chem. Soc. Rev.*, 2022, **51**, 2710–2758, DOI: 10.1039/d1cs00857a.

28 Q. Liu, G. Wen, D. Zhao, L. Xie, S. Sun, L. Zhang, Y. Luo, A. Ali Alshehri, M. S. Hamdy, Q. Kong and X. Sun, Nitrite reduction over Ag nanoarray electrocatalyst for ammonia synthesis, *J. Colloid Interface Sci.*, 2022, **623**, 513–519, DOI: 10.1016/j.jcis.2022.04.173.

29 H. Yin, Y. Peng and J. Li, Electrocatalytic reduction of nitrate to ammonia via a au/cu single atom alloy catalyst, *Environ. Sci. Technol.*, 2023, **57**, 3134–3144, DOI: 10.1021/acs.est.2c07968.

30 S. Yuan, Y. Xue, R. Ma, Q. Ma, Y. Chen and J. Fan, Advances in iron-based electrocatalysts for nitrate reduction, *Sci. Total Environ.*, 2023, **866**, 161444, DOI: 10.1016/j.scitotenv.2023.161444.

31 Q. Liu, L. Xie, J. Liang, Y. Ren, Y. Wang, L. Zhang, L. Yue, T. Li, Y. Luo, N. Li, B. Tang, Y. Liu, S. Gao, A. A. Alshehri, I. Shakir, P. O. Agboola, Q. Kong, Q. Wang, D. Ma and X. Sun, Ambient ammonia synthesis via electrochemical reduction of nitrate enabled by $NiCo_2O_4$ nanowire array, *Small*, 2022, **18**, 2106961, DOI: 10.1002/smll.202106961.

32 X. Li, X. Zhao, Y. Zhou, J. Hu, H. Zhang, X. Hu and G. Hu, Pd nanocrystals embedded in BC_2N for efficient electrochemical conversion of nitrate to ammonia, *Appl. Surf. Sci.*, 2022, **584**, 152556, DOI: 10.1016/j.apsusc.2022.152556.

33 X. Liang, H. Zhu, X. Yang, S. Xue, Z. Liang, X. Ren, A. Liu and G. Wu, Recent advances in designing efficient electrocatalysts for electrochemical nitrate reduction to ammonia, *Small Struct.*, 2023, **4**, 2200202, DOI: 10.1002/sstr.202200202.

34 W. Song, L. Yue, X. Fan, Y. Luo, B. Ying, S. Sun, D. Zheng, Q. Liu, M. S. Hamdy and X. Sun, Recent progress and strategies on the design of catalysts for electrochemical ammonia synthesis from nitrate reduction, *Inorg. Chem. Front.*, 2023, **10**, 3489–3514, DOI: 10.1039/D3QI00554B.

35 M. Teng, J. Ye, C. Wan, G. He and H. Chen, Research progress on Cu-based catalysts for electrochemical nitrate reduction reaction to ammonia, *Ind. Eng. Chem. Res.*, 2022, **61**, 14731–14746, DOI: 10.1021/acs.iecr.2c02495.

36 X. Zhu, X. Fan, H. Lin, S. Li, Q. Zhai, Y. Jiang and Y. Chen, Highly efficient electroenzymatic cascade reduction reaction for the conversion of nitrite to ammonia, *Adv. Energy Mater.*, 2023, **13**, 2300669, DOI: 10.1002/aenm.202300669.

37 X. Zhang, Y. Wang, C. Liu, Y. Yu, S. Lu and B. Zhang, Recent advances in non-noble metal electrocatalysts for nitrate reduction, *Chem. Eng. J.*, 2021, **403**, 126269, DOI: 10.1016/j.cej.2020.126269.

38 Y. Wang, C. Wang, M. Li, Y. Yu and B. Zhang, Nitrate electroreduction: mechanism insight, in situ characterization, performance evaluation and challenges, *Chem. Soc. Rev.*, 2021, **50**, 6720–6733, DOI: 10.1039/D1CS00116G.

39 J. Theerthagiri, J. Park, H. T. Das, N. Rahamathulla, E. S. F. Cardoso, A. P. Murthy, G. Maia, D. V. N. Vo and M. Y. Choi, Electrocatalytic conversion of nitrate waste into ammonia: a review, *Environ. Chem. Lett.*, 2022, **20**, 2929–2949, DOI: 10.1007/s10311-022-01469-y.

40 R. Jia, Y. Wang, C. Wang, Y. Ling, Y. Yu and B. Zhang, Boosting selective nitrate electroreduction to ammonium by constructing oxygen vacancies in TiO_2, *ACS Catal.*, 2020, **10**, 3533–3540, DOI: 10.1021/acscatal.9b05260.

41 J. Long, S. Chen, Y. Zhang, C. Guo, X. Fu, D. Deng and J. Xiao, Direct electrochemical ammonia synthesis from nitric oxide, *Angew. Chem., Int. Ed.*, 2020, **59**, 9711–9718, DOI: 10.1002/anie.202002337.

42 Y. Feng, L. Chen and Z. Yuan, Recent advances in transition metal layered double hydroxide based materials as efficient electrocatalysts, *J. Ind. Eng. Chem.*, 2023, **120**, 27–46, DOI: 10.1016/j.jiec.2022.12.030.

43 Z. Zhao, S. Liu, S. Zha, D. Cheng, F. Studt, G. Henkelman and J. Gong, Theory-guided design of catalytic materials using scaling relationships and reactivity descriptors, *Nat. Rev. Mater.*, 2019, **4**, 792–804, DOI: 10.1038/s41578-019-0152-x.

44 C. Wang, Y. Zhang, H. Luo, H. Zhang, W. Li, W. Zhang and J. Yang, Iron-based nanocatalysts for electrochemical nitrate reduction, *Small Methods*, 2022, **6**, 2200790, DOI: 10.1002/smtd.202200790.

45 Z. Niu, S. Fan, X. Li, Z. Liu, J. Wang, J. Duan, M. O. Tadé and S. Liu, Facile tailoring of the electronic structure and the d-band center of copper-doped cobaltate for efficient nitrate electrochemical hydrogenation, *ACS Appl. Mater. Interfaces*, 2022, **14**, 35477–35484, DOI: 10.1021/acsami.2c04789.

46 S. Hsieh and A. A. Gewirth, Nitrate reduction catalyzed by underpotentially deposited Cd on Au(111): identification of the electroactive surface structure, *Langmuir*, 2000, **16**, 9501–9512, DOI: 10.1021/la000808x.

47 W. Jung and Y. J. Hwang, Material strategies in the electrochemical nitrate reduction reaction to ammonia production, *Mater. Chem. Front.*, 2021, **5**, 6803–6823, DOI: 10.1039/D1QM00456E.

48 P. Yu, F. Wang, T. A. Shifa, X. Zhan, X. Lou, F. Xia and J. He, Earth abundant materials beyond transition metal dichalcogenides: a focus on electrocatalyzing hydrogen evolution reaction, *Nano Energy*, 2019, **58**, 244–276, DOI: 10.1016/j.nanoen.2019.01.017.

49 Z. Fang, Z. Jin, S. Tang, P. Li, P. Wu and G. Yu, Porous two-dimensional iron-cyano nanosheets for high-rate electrochemical nitrate reduction, *ACS Nano*, 2022, **16**, 1072–1081, DOI: 10.1021/acsnano.1c08814.

50 X. Qin, B. Yan, D. Kim, Z. Teng, T. Chen, J. Choi, L. Xu and Y. Piao, Interfacial engineering and hydrophilic/aerophobic tuning of sn4p3/co2p heterojunction nanoarrays for high-efficiency fully reversible water electrolysis, *Appl. Catal., B*, 2022, **304**, 120923, DOI: 10.1016/j.apcatb.2021.120923.

51 H. Jiang, G. Chen, O. Savateev, J. Xue, L. Ding, Z. Liang, M. Antonietti and H. Wang, Enabled efficient ammonia synthesis and energy supply in a zinc nitrate battery system by separating nitrate reduction process into two stages, *Angew. Chem., Int. Ed.*, 2023, **62**, e202218717, DOI: 10.1002/anie.202218717.

52 J. Pérez-Ramírez and N. López, Strategies to break linear scaling relationships, *Nat. Catal.*, 2019, **2**, 971–976, DOI: 10.1038/s41929-019-0376-6.

53 Q. Gao, H. S. Pillai, Y. Huang, S. Liu, Q. Mu, X. Han, Z. Yan, H. Zhou, Q. He, H. Xin and H. Zhu, Breaking adsorption-energy scaling limitations of electrocatalytic nitrate reduction on intermetallic cupd nanocubes by machine-learned insights, *Nat. Commun.*, 2022, **13**, 2338, DOI: 10.1038/s41467-022-29926-w.

54 A. D. Doyle, J. H. Montoya and A. Vojvodic, Improving oxygen electrochemistry through nanoscopic confinement, *ChemCatChem*, 2015, **7**, 709, DOI: 10.1002/cctc.201500103.

55 A. Khorshidi, J. Violet, J. Hashemi and A. A. Peterson, How strain can break the scaling relations of catalysis, *Nat. Catal.*, 2018, **1**, 263–268, DOI: 10.1038/s41929-018-0054-0.

56 J. Chen, X. Chen, Y. Liu, Y. Qiao, S. Guan, L. Li and S. Chou, Recent progress of transition metal-based catalysts as cathodes in O_2/H_2O-involved and pure Li-CO_2 batteries, *Energy Environ. Sci.*, 2023, **16**, 792–829, DOI: 10.1039/D2EE03015B.

57 H. Li, X. Han, W. Zhao, A. Azhar, S. Jeong, D. Jeong, J. Na, S. Wang, J. Yu and Y. Yamauchi, Electrochemical preparation of nano/micron structure transition metal-based catalysts for the oxygen evolution reaction, *Mater. Horiz.*, 2022, **9**, 1788–1824, DOI: 10.1039/D2MH00075J.

58 H. Wang, M. Sun, J. Ren and Z. Yuan, Circumventing challenges: design of anodic electrocatalysts for hybrid water electrolysis systems, *Adv. Energy Mater.*, 2023, **13**, 2203568, DOI: 10.1002/aenm.202203568.

59 M. Yang, Z. Wang, D. Jiao, G. Li, Q. Cai and J. Zhao, Tuning single metal atoms anchored on graphdiyne for highly efficient and selective nitrate electroreduction to ammonia under aqueous environments: a computational study, *Appl. Surf. Sci.*, 2022, **592**, 153213, DOI: 10.1016/j.apsusc.2022.153213.

60 A. S. Fajardo, P. Westerhoff, C. M. Sanchez-Sanchez and S. Garcia-Segura, Earth-abundant elements a sustainable solution for electrocatalytic reduction of nitrate, *Appl. Catal., B*, 2021, **281**, 119465, DOI: 10.1016/j.apcatb.2020.119465.

61 X. Yang, R. Wang, S. Wang, C. Song, S. Lu, L. Fang, F. Yin and H. Liu, Sequential active-site switches in integrated Cu/Fe-TiO_2 for efficient electroreduction from nitrate into ammonia, *Appl. Catal., B*, 2023, **325**, 122360, DOI: **10.1016/j.apcatb.2023.122360**.

62 J. Cai, Y. Wei, A. Cao, J. Huang, Z. Jiang, S. Lu and S. Zang, Electrocatalytic nitrate-to-ammonia conversion with ~100% faradaic efficiency via single-atom alloying, *Appl. Catal., B*, 2022, **316**, 121683, DOI: **10.1016/j.apcatb.2022.121683**.

63 Y. Wang, A. Xu, Z. Wang, L. Huang, J. Li, F. Li, J. Wicks, M. Luo, D. Nam, C. Tan, Y. Ding, J. Wu, Y. Lum, C. Dinh, D. Sinton, G. Zheng and E. H. Sargent, Enhanced nitrate-to-ammonia activity on copper–nickel alloys via tuning of intermediate adsorption, *J. Am. Chem. Soc.*, 2020, **142**, 5702–5708, DOI: **10.1021/jacs.9b13347**.

64 J. Fang, Q. Zheng, Y. Lou, K. Zhao, S. Hu, G. Li, O. Akdim, X. Huang and S. Sun, Ampere-level current density ammonia electrochemical synthesis using cuco nanosheets simulating nitrite reductase bifunctional nature, *Nat. Commun.*, 2022, **13**, 7899, DOI: **10.1038/s41467-022-35533-6**.

65 W. Gao, K. Xie, J. Xie, X. Wang, H. Zhang, S. Chen, H. Wang, Z. Li and C. Li, Alloying of Cu with Ru enabling the relay catalysis for reduction of nitrate to ammonia, *Adv. Mater.*, 2023, **35**, 2202952, DOI: **10.1002/adma.202202952**.

66 T. Hu, C. Wang, M. Wang, C. M. Li and C. Guo, Theoretical insights into superior nitrate reduction to ammonia performance of copper catalysts, *ACS Catal.*, 2021, **11**, 14417–14427, DOI: **10.1021/acscatal.1c03666**.

67 J. Qin, L. Chen, K. Wu, X. Wang, Q. Zhao, L. Li, B. Liu and Z. Ye, Electrochemical synthesis of ammonium from nitrates via surface engineering in Cu_2O (100) facets, *ACS Appl. Energy Mater.*, 2022, **5**, 71–76, DOI: **10.1021/acsaem.1c02319**.

68 A. Yz, L. B. Yang, A. Zz, B. Zm, B. Cw and B. Sga, Flower-like open-structured polycrystalline copper with synergistic multi-crystal plane for efficient electrocatalytic reduction of nitrate to ammonia, *Nano Energy*, 2022, **97**, 107124, DOI: **10.1016/j.nanoen.2022.107124**.

69 Y. Fu, S. Wang, Y. Wang, P. Wei, J. Shao, T. Liu, G. Wang and X. Bao, Enhancing electrochemical nitrate reduction to ammonia over Cu nanosheets via facet tandem catalysis, *Angew. Chem., Int. Ed.*, 2023, **62**, e202303327, DOI: **10.1002/anie.202303327**.

70 Q. Hu, Y. Qin, X. Wang, Z. Wang, X. Huang, H. Zheng, K. Gao, H. Yang, P. Zhang and M. Shao, Reaction intermediate-mediated electrocatalyst synthesis favors specified facet and defect exposure for efficient nitrate-ammonia conversion, *Energy Environ. Sci.*, 2021, **14**, 4989–4997, DOI: **10.1039/D1EE01731D**.

71 W. Zhong, Z. Gong, Z. He, N. Zhang, X. Kang, X. Mao and Y. Chen, Modulating surface oxygen species via facet engineering for efficient conversion of nitrate to ammonia, *J. Energy Chem.*, 2023, **78**, 211–221, DOI: **10.1016/j.jechem.2022.11.024**.

72 T. Zhu, Q. Chen, P. Liao, W. Duan, S. Liang, Z. Yan and C. Feng, Single-atom Cu catalysts for enhanced electrocatalytic nitrate reduction with significant alleviation of nitrite production, *Small*, 2020, **16**, 2004526, DOI: **10.1002/smll.202004526**.

73 Y. Bu, C. Wang, W. Zhang, X. Yang, J. Ding and G. Gao, Electrical pulse-driven periodic self-repair of Cu-Ni tandem catalyst for efficient ammonia synthesis from nitrate, *Angew. Chem., Int. Ed.*, 2023, **62**, e202217337, DOI: **10.1002/anie.202217337**.

74 Y. Zhang, Y. Wang, L. Han, S. Wang, T. Cui, Y. Yan, M. Xu, H. Duan, Y. Kuang and X. Sun, Nitrite electroreduction to ammonia promoted by molecular carbon dioxide with near-unity faradaic efficiency, *Angew. Chem.*, 2023, **135**, 202213711, DOI: **10.1002/anie.202213711**.

75 Q. Liu, Y. Peng, Y. Zhao, Q. Zhao, X. Li, Q. Zhang, J. Sui, C. Wang and J. Li, Excellent anammox performance driven by stable partial denitrification when encountering seasonal decreasing temperature, *Bioresour. Technol.*, 2022, **364**, 128041, DOI: **10.1016/j.biortech.2022.128041**.

76 P. Li, Z. Jin, Z. Fang and G. Yu, A single-site iron catalyst with preoccupied active centers that achieves selective ammonia electrosynthesis from nitrate, *Energy Environ. Sci.*, 2021, **14**, 3522–3531, DOI: **10.1039/D1EE00545F**.

77 L. Li, K. Yuan and Y. Chen, Breaking the scaling relationship limit: from single-atom to dual-atom catalysts, *Acc. Mater. Res.*, 2022, **3**, 584–596, DOI: **10.1021/accountsmr.1c00264**.

78 Z. Shu, H. Chen, X. Liu, H. Jia, H. Yan and Y. Cai, High-throughput screening of heterogeneous transition metal dual-atom catalysts by synergistic effect for nitrate reduction to ammonia, *Adv. Funct. Mater.*, 2023, 2301493, DOI: **10.1002/adfm.202301493**.

79 J. Wang, Y. Wang, C. Cai, Y. Liu, D. Wu, M. Wang, M. Li, X. Wei, M. Shao and M. Gu, Cu-doped iron oxide for the efficient electrocatalytic nitrate reduction reaction, *Nano Lett.*, 2023, **23**, 1897–1903, DOI: **10.1021/acs.nanolett.2c04949**.

80 H. Zhang, C. Wang, H. Luo, J. Chen, M. Kuang and J. Yang, Iron nanoparticles protected by chainmail-structured graphene for durable electrocatalytic nitrate reduction to nitrogen, *Angew. Chem., Int. Ed.*, 2023, **62**, e202217071, DOI: **10.1002/anie.202217071**.

81 N. C. Kani, J. A. Gauthier, A. Prajapati, J. Edgington, I. Bordawekar, W. Shields, M. Shields, L. C. Seitz, A. R. Singh and M. R. Singh, Solar-driven electrochemical synthesis of ammonia using nitrate with 11% solar-to-fuel efficiency at ambient conditions, *Energy Environ. Sci.*, 2021, **14**, 6349–6359, DOI: **10.1039/D1EE01879E**.

82 W. Lin, E. Zhou, J. Xie, J. Lin and Y. Wang, A high power density Zn-nitrate electrochemical cell based on theoretically screened catalysts, *Adv. Funct. Mater.*, 2022, **32**, 2209464, DOI: **10.1002/adfm.202209464**.

83 J. Wang, C. Cai, Y. Wang, X. Yang, D. Wu, Y. Zhu, M. Li, M. Gu and M. Shao, Electrocatalytic reduction of nitrate to ammonia on low-cost ultrathin CoO_x nanosheets, *ACS Catal.*, 2021, **11**, 15135–15140, DOI: **10.1021/acscatal.1c03918**.

84 Y. Feng, J. Ren, H. Wang, L. Wang and Z. Yuan, Core-shell heterojunction engineering of Co_3O_4/NiFe LDH nanosheets as bifunctional electrocatalysts for efficient reduction of nitrite to ammonia, *Inorg. Chem. Front.*, 2023, **10**, 4510–4518, DOI: **10.1039/D3QI00795B**.

85 S. Ye, Z. Chen, G. Zhang, W. Chen, C. Peng, X. Yang, L. Zheng, Y. Li, X. Ren, H. Cao, D. Xue, J. Qiu, Q. Zhang and J. Liu, Elucidating the activity, mechanism and application of selective electrosynthesis of ammonia from nitrate on cobalt phosphide, *Energy Environ. Sci.*, 2022, **15**, 760–770, DOI: **10.1039/D1EE03097C**.

86 G. Wen, J. Liang, Q. Liu, T. Li, X. An, F. Zhang, A. A. Alshehri, K. A. Alzahrani, Y. Luo, Q. Kong and X. Sun, Ambient ammonia production via electrocatalytic nitrite reduction catalyzed by a CoP nanoarray, *Nano Res.*, 2022, **15**, 972–977, DOI: **10.1007/s12274-021-3583-9**.

87 S. Han, H. Li, T. Li, F. Chen, R. Yang, Y. Yu and B. Zhang, Ultralow overpotential nitrate reduction to ammonia via a three-step relay mechanism, *Nat. Catal.*, 2023, **6**, 402–414, DOI: **10.1038/s41929-023-00951-2**.

88 O. Q. Carvalho, R. Marks, H. K. K. Nguyen, M. E. Vitale-Sullivan, S. C. Martinez, L. árnadóttir and K. A. Stoerzinger, Role of electronic structure on nitrate reduction to ammonium: a periodic journey, *J. Am. Chem. Soc.*, 2022, **144**, 14809–14818, DOI: **10.1021/jacs.2c05673**.

89 Y. Luo, Z. Zhang, F. Yang, J. Li, Z. Liu, W. Ren, S. Zhang and B. Liu, Stabilized hydroxide-mediated nickel-based electrocatalysts for high-current-density hydrogen evolution in alkaline media, *Energy Environ. Sci.*, 2021, **14**, 4610–4619, DOI: **10.1039/D1EE01487K**.

90 J. Ren, L. Chen, W. Tian, X. Song, Q. Kong, H. Wang and Z. Yuan, Rational synthesis of core-shell-structured nickel sulfide-based nanostructures for efficient seawater electrolysis, *Small*, 2023, 2300194, DOI: **10.1002/smll.202300194**.

91 Y. Tian, A. Huang, Z. Wang, M. Wang, Q. Wu, Y. Shen, Q. Zhu, Y. Fu and M. Wen, Two-dimensional hetero-nanostructured electrocatalyst of Ni/NiFe-layered double oxide for highly efficient hydrogen evolution reaction in alkaline medium, *Chem. Eng. J.*, 2021, **426**, 131827, DOI: **10.1016/j.cej.2021.131827**.

92 Z. Wenxiao, Z. Liuyi, Y. Zhang, L. Zichao, L. Zhenchao, Z. Yifan, X. Haolin, D. Zhi, W. Chaohai and F. Chunhua, Self-activated ni cathode for electrocatalytic nitrate reduction to ammonia: from fundamentals to scale-up for treatment of industrial wastewater, *Environ. Sci. Technol.*, 2021, **55**, 13231–13243, DOI: **10.1021/acs.est.1c02278**.

93 J. Zhou, M. Wen, R. Huang, Q. Wu, Y. Luo, Y. Tian, G. Wei and Y. Fu, Regulating active hydrogen adsorbed on grain boundary defects of nano-nickel for boosting ammonia electrosynthesis from nitrate, *Energy Environ. Sci.*, 2023, **16**, 2611–2620, DOI: **10.1039/D2EE04095F**.

94 Z. Cai, C. Ma, D. Zhao, X. Fan, R. Li, L. Zhang, J. Li, X. He, Y. Luo, D. Zheng, Y. Wang, B. Ying, S. Sun, J. Xu, Q. Lu and X. Sun, Ni doping enabled improvement in electrocatalytic nitrite-to-ammonia conversion over TiO_2 nanoribbon, *Mater. Today Energy*, 2023, **31**, 101220, DOI: **10.1016/j.mtener.2022.101220**.

95 L. Chen, X. Song, J. Ren and Z. Yuan, Precisely modifying Co_2P/black TiO_2 S-scheme heterojunction by in situ formed P and C dopants for enhanced photocatalytic H_2 production, *Appl. Catal., B*, 2022, **315**, 121546, DOI: **10.1016/j.apcatb.2022.121546**.

96 L. Ouyang, X. He, S. Sun, Y. Luo, D. Zheng, J. Chen, Y. Li, Y. Lin, Q. Liu, A. M. Asiri and X. Sun, Enhanced electrocatalytic nitrite reduction to ammonia over P-doped TiO_2 nanobelt array, *J. Mater. Chem. A*, 2022, **10**, 23494–23498, DOI: **10.1039/D2TA06933D**.

97 Q. Li, Y. Liu, Z. Wan, H. Cao, S. Zhang, Y. Zhou, X. Ye, X. Liu and D. Zhang, Microwave-assisted synthesis of oxygen vacancy associated TiO_2 for efficient photocatalytic nitrate reduction, *Chin. Chem. Lett.*, 2022, **33**, 3835–3841, DOI: **10.1016/j.cclet.2021.12.025**.

98 H. Wang, F. Zhang, M. Jin, D. Zhao, X. Fan, Z. Li, Y. Luo, D. Zheng, T. Li, Y. Wang, B. Ying, S. Sun, Q. Liu, X. Liu and X. Sun, V-doped TiO_2 nanobelt array for high-efficiency electrocatalytic nitrite reduction to ammonia, *Mater. Today Phys.*, 2023, **30**, 100944, DOI: **10.1016/j.mtphys.2022.100944**.

99 J. Nowotny, M. A. Alim, T. Bak, M. A. Idris, M. Ionescu, K. Prince, M. Z. Sahdan, K. Sopian, M. A. Mat Teridi and W. Sigmund, Defect chemistry and defect engineering of TiO_2-based semiconductors for solar energy conversion, *Chem. Soc. Rev.*, 2015, **44**, 8424–8442, DOI: **10.1039/C4CS00469H**.

100 J. Liu, X. Yang, F. Si, B. Zhao, X. Xi, L. Wang, J. Zhang, X. Fu and J. Luo, Interfacial component coupling effects towards precise heterostructure design for efficient electrocatalytic water splitting, *Nano Energy*, 2022, **103**, 107753, DOI: **10.1016/j.nanoen.2022.107753**.

101 Y. Liu, J. Guo, E. Zhu, L. Liao, S. Lee, M. Ding, I. Shakir, V. Gambin, Y. Huang and X. Duan, Approaching the schottky-mott limit in van der Waals metal-semiconductor junctions, *Nature*, 2018, **557**, 696–700, DOI: **10.1038/s41586-018-0129-8**.

102 X. Fan, D. Zhao, Z. Deng, L. Zhang, J. Li, Z. Li, S. Sun, Y. Luo, D. Zheng, Y. Wang, B. Ying, J. Zhang, A. A. Alshehri, Y. Lin, C. Tang, X. Sun and Y. Zheng, Constructing Co@TiO_2 nanoarray heterostructure with schottky contact for selective electrocatalytic nitrate reduction to ammonia, *Small*, 2023, **19**, 2208036, DOI: **10.1002/smll.202208036**.

103 Z. Deng, C. Ma, X. Fan, Z. Li, Y. Luo, S. Sun, D. Zheng, Q. Liu, J. Du, Q. Lu, B. Zheng and X. Sun, Construction of CoP/TiO_2 nanoarray for enhanced electrochemical nitrate reduction to ammonia, *Mater. Today Phys.*, 2022, **28**, 100854, DOI: **10.1016/j.mtphys.2022.100854**.

104 J. Yang, H. Qi, A. Li, X. Liu, X. Yang, S. Zhang, Q. Zhao, Q. Jiang, Y. Su, L. Zhang, J. Li, Z. Tian, W. Liu, A. Wang and T. Zhang, Potential-driven restructuring of Cu single atoms to nanoparticles for boosting the electrochemical reduction of nitrate to ammonia, *J. Am. Chem. Soc.*, 2022, **144**, 12062–12071, DOI: **10.1021/jacs.2c02262**.

105 X. Fu, X. Zhao, X. Hu, K. He, Y. Yu, T. Li, Q. Tu, X. Qian, Q. Yue, M. R. Wasielewski and Y. Kang, Alternative route for electrochemical ammonia synthesis by reduction of nitrate on copper nanosheets, *Appl. Mater. Today*, 2020, **19**, 100620, DOI: **10.1016/j.apmt.2020.100620**.

106 Y. Xu, Y. Wen, T. Ren, H. Yu, K. Deng, Z. Wang, X. Li, L. Wang and H. Wang, Engineering the surface chemical microenvironment over cuo nanowire arrays by polyaniline modification for efficient ammonia electrosynthesis from nitrate, *Appl. Catal., B*, 2023, **320**, 121981, DOI: **10.1016/j.apcatb.2022.121981**.

107 T. Ren, K. Ren, M. Wang, M. Liu, Z. Wang, H. Wang, X. Li, L. Wang and Y. Xu, Concave-convex surface oxide layers over copper nanowires boost electrochemical nitrate-to-ammonia conversion, *Chem. Eng. J.*, 2021, **426**, 130759, DOI: **10.1016/j.cej.2021.130759**.

108 L. Ouyang, X. Fan, Z. Li, X. He, S. Sun, Z. Cai, Y. Luo, D. Zheng, B. Ying, J. Zhang, A. A. Alshehri, Y. Wang, K. Ma and X. Sun, High-efficiency electroreduction of nitrite to ammonia on a Cu@TiO_2 nanobelt array, *Chem. Commun.*, 2023, **59**, 1625–1628, DOI: **10.1039/D2CC06261E**.

109 Q. Chen, X. An, Q. Liu, X. Wu, L. Xie, J. Zhang, W. Yao, M. S. Hamdy, Q. Kong and X. Sun, Boosting electrochemical nitrite-ammonia conversion properties by a Cu foam@Cu_2O catalyst, *Chem. Commun.*, 2022, **58**, 517–520, DOI: **10.1039/D1CC06215H**.

110 J. Liang, B. Deng, Q. Liu, G. Wen, Q. Liu, T. Li, Y. Luo, A. A. Alshehri, K. A. Alzahrani, D. Ma and X. Sun, High-efficiency electrochemical nitrite reduction to ammonium using a Cu_3P nanowire array under ambient conditions, *Green Chem.*, 2021, **23**, 5487–5493, DOI: **10.1039/D1GC01614H**.

111 T. Zhao, X. Li, J. Hu, J. Zhou, X. Jia and G. Hu, P-doped $FeCo_2O_4$ *in situ* decorated on carbon cloth as robust electrocatalysts for reducing nitrate and nitrite to ammonia, *J. Environ. Chem. Eng.*, 2023, **11**, 110122, DOI: **10.1016/j.jece.2023.110122**.

112 J. Yuan, H. Yin, X. Jin, D. Zhao, Y. Liu, A. Du, X. Liu and A. P. O. Mullane, A practical FeP nanoarrays electrocatalyst for efficient catalytic reduction of nitrite ions in wastewater to ammonia, *Appl. Catal., B*, 2023, **325**, 122353, DOI: **10.1016/j.apcatb.2022.122353**.

113 X. Li, Z. Li, L. Zhang, D. Zhao, J. Li, S. Sun, L. Xie, Q. Liu, A. A. Alshehri, Y. Luo, Y. Liao, Q. Kong and X. Sun, Ni nanoparticle-decorated biomass carbon for efficient electrocatalytic nitrite reduction to ammonia, *Nanoscale*, 2022, **14**, 13073–13077, DOI: **10.1039/D2NR03540E**.

114 C. Wang, W. Zhou, Z. Sun, Y. Wang, B. Zhang and Y. Yu, Integrated selective nitrite reduction to ammonia with tetrahydroisoquinoline semi-dehydrogenation over a vacancy-rich ni bifunctional electrode, *J. Mater. Chem. A*, 2021, **9**, 239–243, DOI: **10.1039/D0TA09590G**.

115 Q. Song, S. Zhang, X. Hou, J. Li, L. Yang, X. Liu and M. Li, Efficient electrocatalytic nitrate reduction via boosting oxygen vacancies of TiO_2 nanotube array by highly dispersed trace Cu doping, *J. Hazard. Mater.*, 2022, **438**, 129455, DOI: **10.1016/j.jhazmat.2022.129455**.

116 Z. Cai, D. Zhao, X. Fan, L. Zhang, J. Liang, Z. Li, J. Li, Y. Luo, D. Zheng, Y. Wang, T. Li, H. Yan, B. Ying, S. Sun, A. A. Alshehri, H. Yan, J. Xu, Q. Kong and X. Sun, Rational construction of heterostructured Cu_3P@TiO_2 nanoarray for high-efficiency electrochemical nitrite reduction to ammonia, *Small*, 2023, 2300620, DOI: **10.1002/smll.202300620**.